# Physicochemical and Electronic Properties of Cationic [6]Helicenes, from Chemical and Electrochemical Stabilities to Far-Red (Polarized) Luminescence

Johann Bosson, Geraldine M. Labrador, Simon Pascal, François-Alexandre Miannay, Oleksandr Yushchenko, Haidong Li, Laurent Bouffier, Neso Sojic, Roberto C. Tovar, Gilles Muller, Denis Jacquemin, Adèle D. Laurent, Boris Le Guennic, Eric Vauthey,* Jérôme Lacour*

## Electronic Supporting Information

# 1    Determination of the p$K_{R+}$ values of [6]helicenes 1, 2 and 3

The p$K_{R+}$ values of **1** was determined in aqueous solution, whereas the p$K_{R+}$ values of **2** and **3** were determined using the technics developed by Laursen and co-workers.[1,2] Measurements were performed on a V-650 UV-Vis Spectrophotometer (JASCO) at a controlled temperature of 20 °C in 2 mL quartz cells equipped with a Teflon cap (QS from HELLMA ANALYTICS, 1 cm optical path) under $N_2$ atmosphere. Each measure (baseline, absorption without and with base) has been repeated at least twice, reported data being the average of two convergent measurements. The p$K_{R+}$ values were determined at the $\lambda_{max}$ wavelength (without the base), that is 564 nm for **1**, 574 nm for **2** and 619 nm for **3**.

DMSO was distilled on $CaH_2$ under reduced pressure under $N_2$ atmosphere, degassed using freeze-pumping technics (x 3) and stored on 4 Å molecular sieves under $N_2$ atmosphere. Milli Q water was degassed using freeze-pumping technics (x 3) and stored under $N_2$ atmosphere. In the following, "DMSO" and "$H_2O$" refer to the distilled and degassed solutions.

A 0.1 M solution of $[Me_4N]^+[OH]^-$ in $H_2O$ was prepared by diluting 360 µL of a solution of 25 % wt. $[Me_4N]^+[OH]^-$ in $H_2O$ (FLUKA) into 9.64 mL $H_2O$.

## 1.1    Dioxa [6]helicene 1

0.1 M sodium borate buffered aqueous solution was prepared by dissolving 3.82 g of $Na_2B_4O_7.10H_2O$ (borax) in 100 mL $H_2O$. The buffered solution was then degassed using freeze-pumping technics (x 3). pH values were then adjusted with 5 N NaOH aqueous solution of 7 N HCl aqueous solution. pH values of the solutions (6.11, 8.06, 9.08, 10.04 and 11.11) were verified on a FE20 pH meter (METTLER TOLEDO) at 20 °C. Separately, a $10^{-3}$ M solution of **1** in distilled and degassed DMSO was prepared (0.46 mg in 1000 µL).

Measurements proceeded as follows: 2000 µL of the appropriate buffered solution was charged in the cell. Baseline was recorded. Then 20 µL of the $10^{-3}$ M solution of **1** DMSO was added to the cell through the septum (final concentration at $10^{-5}$ M) and absorption was recorded immediately (Figure S1).
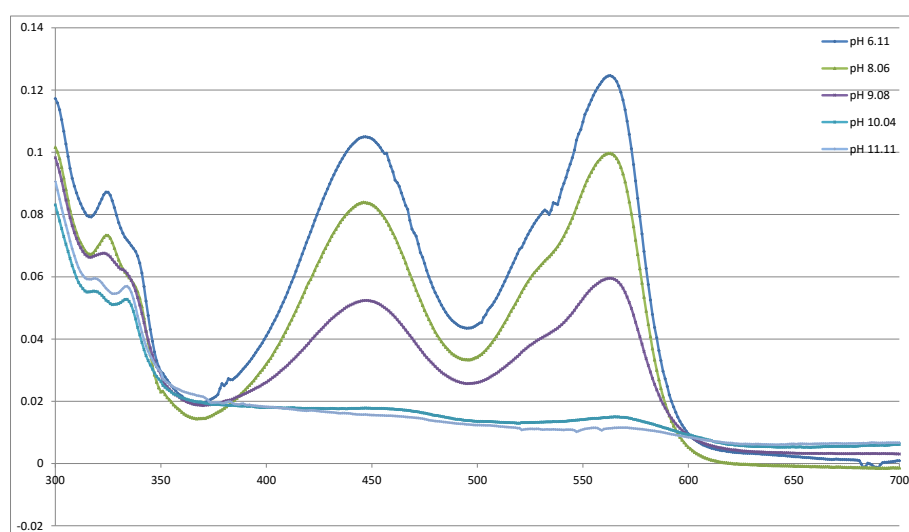
Figure S1. UV-Vis absorption spectra (row data) of **1** at different pH.

From those data, log([ROH]/[R$^+$]) were calculated (since log([ROH]/[R$^+$]) = log(A$_0$/A)) and were plotted *vs.* pH (Figure S2).
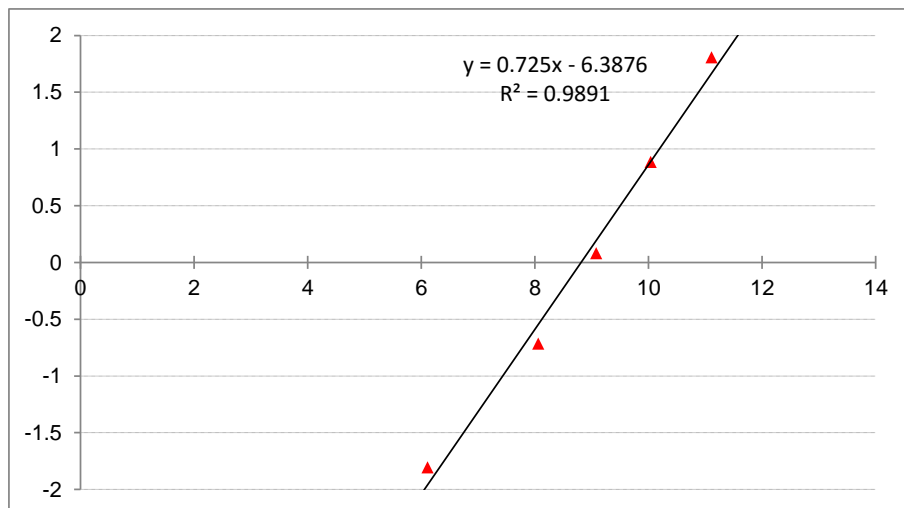


$$y = 0.725x - 6.3876$$
$$R^2 = 0.9891$$

Figure S2. Plot of log([ROH]/[R$^+$]) vs. pH for **1**.

From this plot, a p$K_{R+}$ value of 8.8 was calculated for **1**.

## 1.2   Azaoxa [6]helicene 2

A solution of **2** (2 10$^{-3}$ M) in DMSO (1.00 mg in 1000 μL) was prepared.

Measurements proceeded as follows:

- determination of the A$_0$ values: the quartz cells equipped with a Teflon cap was charged with DMSO and H$_2$O so that the overall volume was 1600 μL. To this mixture was added 200 μL of H$_2$O. The baseline was recorded. Then 18 μL of the 2 10$^{-3}$ M solution of **2** in DMSO (final concentration of 2 10$^{-5}$ M) were added and the A$_0$ values were recorded.

- determination of the A values: this was done following the same procedure as for the determination of the A$_0$ values, excepts that the 200 μL of H$_2$O were replaced by 200 μL of 0.1 M solution of [Me$_4$N]$^+$[OH]$^-$ in H$_2$O and that no baseline was recorded (Figure S3).

Measurements were performed for DMSO/H$_2$O ratios of 900:700, 1000:600, 1100:500 and 1200:400, corresponding to C_ values of 14.86, 15.44, 16.04 and 16.73 respectively.
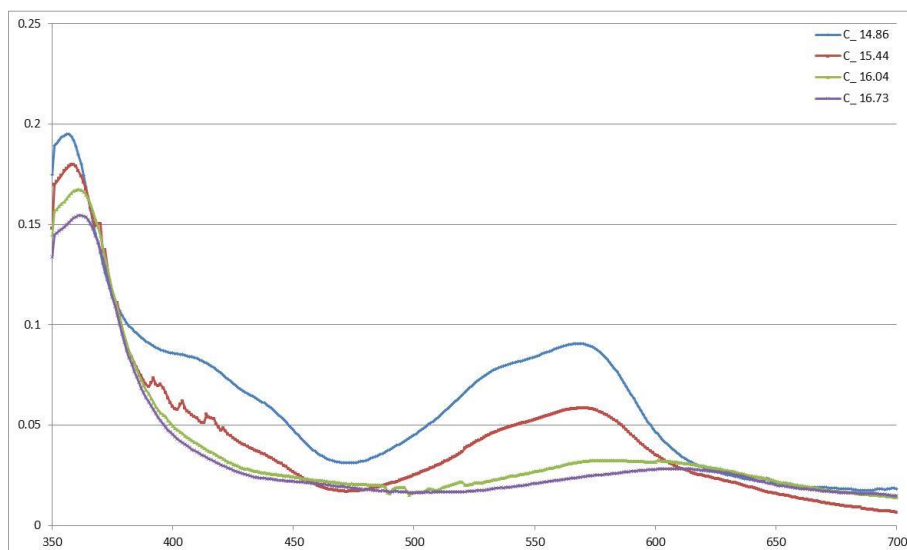
Figure S3. UV-Vis absorption spectra (row data) of **2** at different C_ values.

From those data, log([ROH]/[R$^+$]) were calculated (since log([ROH]/[R$^+$]) = log($A_0$/A)) and were plotted *vs.* C_ (Figure S4). This allowed for the determination of a p$K_{R+}$ value of 15.2 for **2**.

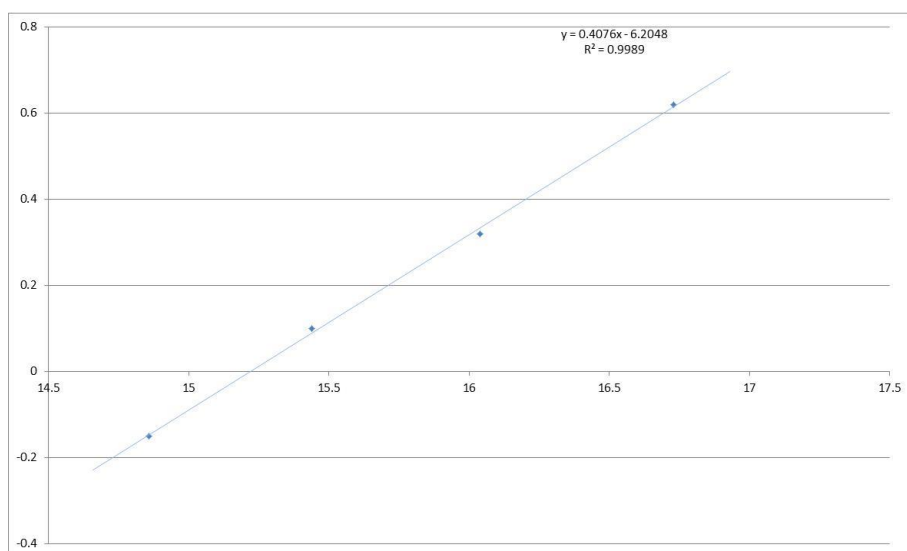

Figure S4. Plot of log([ROH]/[R$^+$]) *vs.* C_ for **2**.

Upon standing, basic solutions of **2** turned slightly blue, indicating the conversion to another dye (Figure S5 at a C_ value of 16.73). This most probably accounts for a slope of log([ROH]/[R$^+$]) *vs.* C_ plotting different from unity. However, upon acidification with conc. HCl just after the measurements, a UV-Vis absorption spectrum similar to the one of the A0 value was obtained.
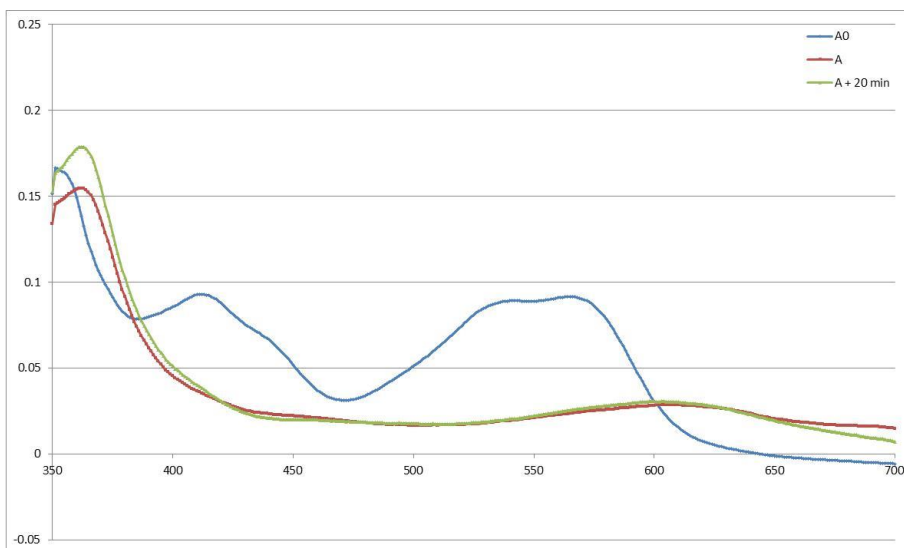
Figure S5. UV-Vis absorption spectra (row data) of **2** in DMSO/$H_2O$ 1200:600 ($A_0$), in solution at C_ = 16.73 (A) and the same cuvette after 20 min standing (A + 20 min).

## 1.3   Diaza [6]helicene 3

A solution of **3** ($2 \ 10^{-3}$ M) in DMSO (1.80 mg in 1000 µL) was prepared.

In the case of C_ values of 19.56, 20.25, and 21.06, measurements were performed using the same methodology as for **2** (*vide supra*).

Measurements were performed for DMSO/$H_2O$ ratios of 1500:100, 1550:50, 1600:00 and 1200:400, corresponding to C_ values of 19.56, 20.25, and 21.06 respectively.

In the case of a C_ value of 21.52, measurements were performed as follow:

A 0.3 M solution of [Me_4N]$^+$[OH]$^-$ in $H_2O$ was prepared by diluting 540 µL of a solution of 25 % wt. [Me_4N]$^+$[OH]$^-$ in $H_2O$ (FLUKA) into 4.46 mL $H_2O$.

- determination of the $A_0$ value: the quartz cells equipped with a Teflon cap was charged with DMSO (1600 µL) and $H_2O$ (200 µL). The baseline was recorded. Then 18 µL of the $2 \ 10^{-3}$ M solution of **2** in DMSO (final concentration of $2 \ 10^{-5}$ M) were added and the $A_0$ values were recorded.

- determination of the A value: this was done following the same procedure as for the determination of the $A_0$ value, excepts that the 200 µL of $H_2O$ were replaced by 200 µL of 0.3 M solution of [Me_4N]$^+$[OH]$^-$ in $H_2O$ and that no baseline was recorded (Figure S6).
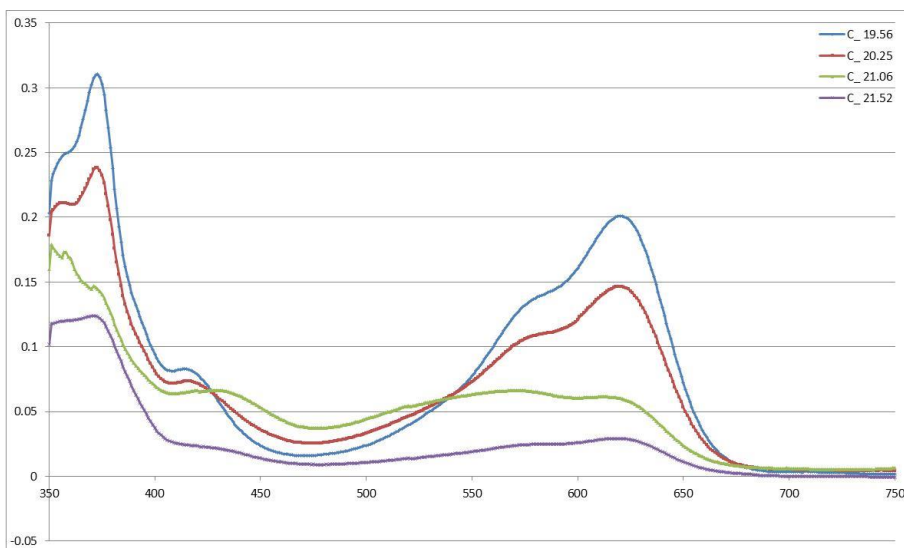
Figure S6. UV-Vis absorption spectra (row data) of **3** at different C_ values.

A clear reduction of the absorption intensities was observed going from C_ 19.56 to C_ 21.06. The formation of 2 isosbestic points could be observed at 428 and 540 nm, indicating the conversion into another dye. This most probably accounts for a slope in the log([ROH]/[R$^+$]) *vs.* C_ plotting different from unity. However, upon acidification with conc. HCl just after the measurements, UV-Vis absorption spectra similar to the ones of the A0 value were obtained.

From those data, log([ROH]/[R$^+$]) were calculated plotted *vs.* C_ (Figure S7). This allowed for the determination of a p$K_{R+}$ value of 20.4 for **2**.
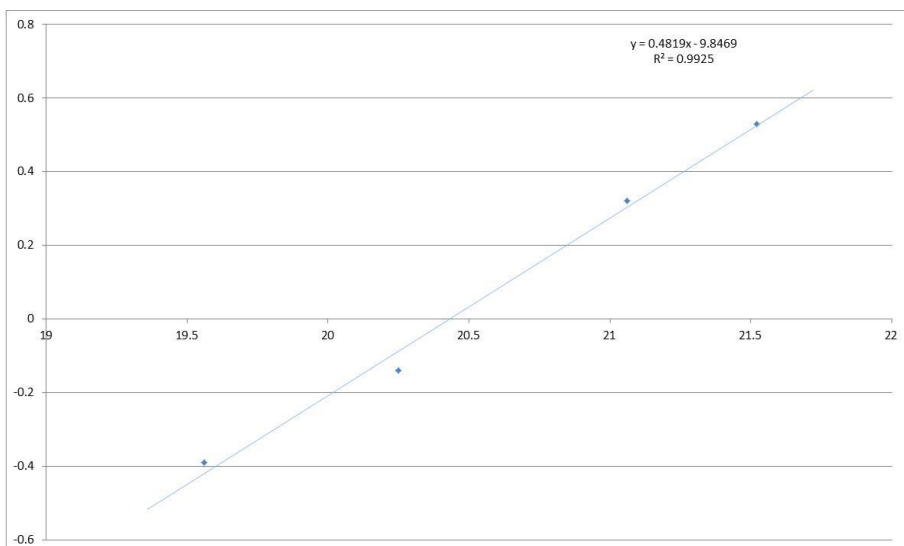


Figure S7. Plot of log([ROH]/[R$^+$]) *vs.* C_ for **3**.

Upon standing, basic solutions of **3** turned slightly pink but UV-Vis absorption spectra similar to the ones of the A0 value could not be obtained upon acidification. UV-Vis spectra clearly showed the irreversible formation of another compound (Figure S8 at C_ = 20.25). This new compound could not be identified.
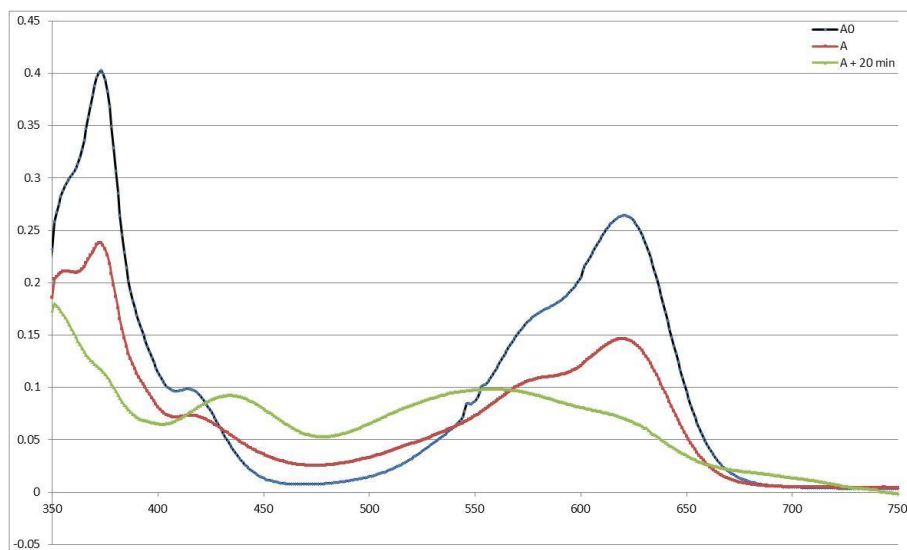
Figure S8. UV-Vis absorption spectra (row data) of **3** in DMSO/$H_2O$ 1750:50 ($A_0$), in solution at C_ = 20.25 (A) and the same cuvette after 20 min standing (A + 20 min).

# 2 Optical properties

## 2.1 Experimental details

### 2.1.1 Steady-state measurements

The electronic absorption and emission spectra have been measured using a Cary 50 spectrometer and a Fluoromax 4 JOBIN-YVON spectrofluorometer, respectively. The fluorescence quantum yields were determined using oxazine 1 in ethanol, sulforhodamine 101 in ethanol and cresyl violet in methanol as references.

### 2.1.2 Time resolved spectroscopy

*Time-resolved fluorescence.* Fluorescence dynamics on the nanosecond time-scale was measured using a time-correlated single photon counting (TCSPC) setup described in details previously.[3,4] Excitation was performed at 395 and 469 nm using ~60 ps pulses at 10 MHz produced by laser diodes (Picoquant, LDH-PC-400 and 470). The full width at half maximum (fwhm) of the instrument response function (irf) was around 200 ps. Faster dynamics was investigated by fluorescence up-conversion (FU) using the same setup as in ref.[5,6]. Excitation was performed at 450 nm using 100 fs pulses produced by frequency doubling the output of a Ti:Sapphire oscillator (Spectra-Physics, Mai Tai). The pump intensity on the sample was around 5 $\mu$J/cm2 and the fwhm of the irf was *ca.* 200 fs. The sample solutions were located in a 0.4 mm rotating cell and had an absorbance of about 0.1 at the excitation wavelength.

*Transient absorption (TA) spectroscopy.* TA measurements were performed with two pump-probe setups. The fs-ps TA setup used to record spectra up to 1.8 ns with an irf of ca. 150 fs (fwhm) has been described in detail elsewhere.[7,8] Excitation was performed using 400 nm pulses generated by frequency doubling part of the output of a standard 1 kHz Ti:Sapphire amplified system. The intensity of the pump pulses on the sample was *ca.* 0.5 mJ/cm$^2$. The ns-$\mu$s TA setup, used to record spectra up to 1 $\mu$s with an irf of 370 ps (fwhm) is the same as that described in ref.[9,10]. Excitation was performed either at 355 nm using a passively Q-switched, frequency doubled or tripled Nd:YAG lasers (Teem Photonics, Powerchip PNG-M02010, Powerchip NanoUV) producing pulses at 500 Hz repetition rate, with approx. 20 $\mu$J energy per pulse, and 300 ps duration. The pump intensity on the sample was also around 0.5 mJ/cm$^2$. In both TA setups, probing was achieved using white light pulses generated by focusing 800 nm pulses in a CaF$_2$ plate and polarised at magic angle relative to the pump pulses. The sample solutions were located in a 1 mm quartz cell and were continuously stirred by N$_2$ bubbling. Their absorbance at the excitation wavelength was around 0.1.

## 2.2 Absorption, Emission and Excitation spectra of compounds 1, 2 and 3
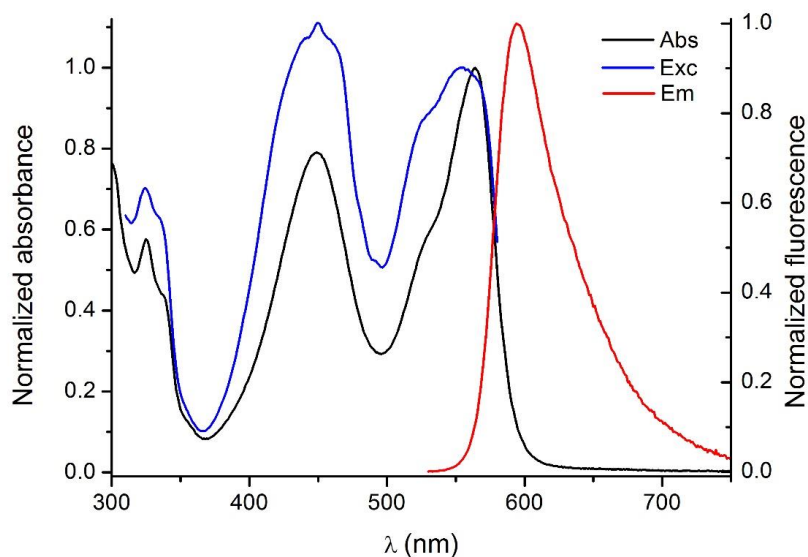
### 2.2.1 Dioxa [6]helicene 1



Figure S9. Normalized absorption (black), excitation (blue, recorded at 595 nm) and emission (red) spectra of dioxa [6]helicene **1**.
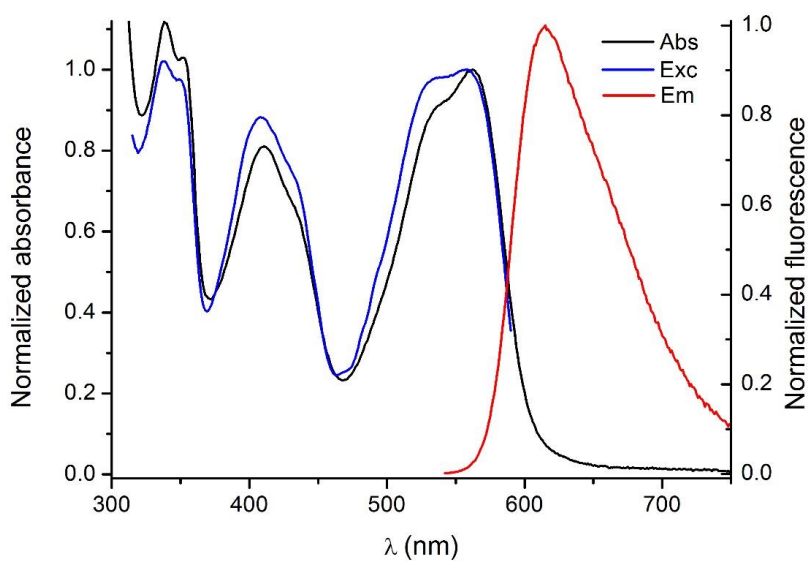
### 2.2.2 Azaoxa [6]helicene 2



Figure S10. Normalized absorption (black), excitation (blue, recorded at 595 nm) and emission (red) spectra of azaoxa [6]helicene **2**.
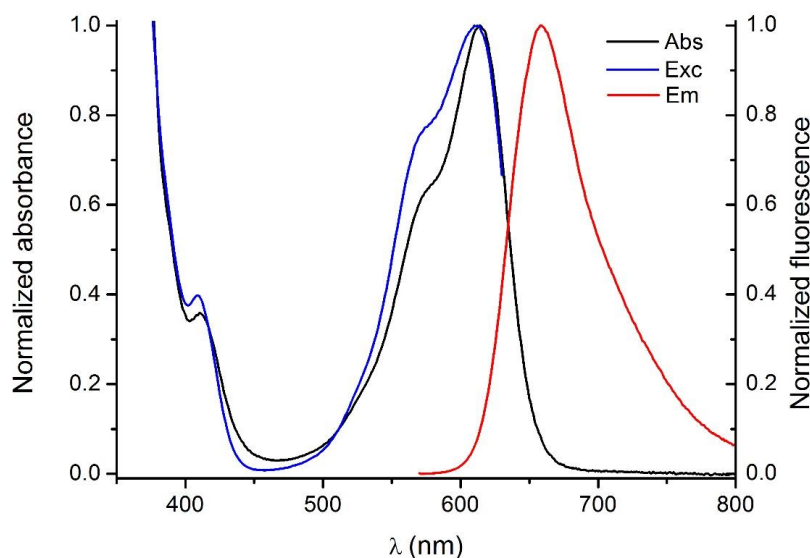
### 2.2.3 Diaza [6]helicene 3



Figure S11. Normalized absorption (black), excitation (blue, recorded at 658 nm) and emission (red) spectra of diaza [6]helicene **3**.

## 2.3 Solvatochromism of compounds 1, 2 and 3

### 2.3.1 Dioxa [6]helicene 1

The behavior of dioxa [6]helicene **1** is different from azaoxa **2** and diaza **3** systems (*vide infra*), as it was found that the use of THF, MeOH and pentanol (PentOH) induced a fading of the color of the chromophore in solution and a quenching of the fluorescence. This is in line with the lower stability as cationic structure of this entity as depicted by the lower $pK_{R+}$ value (*vide supra*). This could be attributed to a nucleophilic attack on the central carbon atom but was not further investigated. Optical properties are gathered in Table S1

| Entry | Solvent | $\varepsilon_r$ | $\lambda_{abs}$ (nm) | $\varepsilon$ (mol$^{-1}$.L.cm$^{-1}$) | $\lambda_{emm}$ (nm) | $\varphi_{fluo}$ (%) | $\tau$ (ns) |
|---|---|---|---|---|---|---|---|
| 1 | CH$_3$CN | 37.5 | 562 | 15480 | 595 | 9.0 | 4.0 |
| 2 | CH$_2$Cl$_2$ | 9 | 573 | 17700 | 592 | 44.5 | 10.5 |
| 3 | CHCl$_3$ | 4.8 | 571 | 16600 | 595 | 24.0 | 8.0 |
| 4 | THF | 7.5 | -$^a$ | -$^a$ | -$^a$ | -$^a$ | -$^a$ |
| 5 | DMSO | 46.7 | 566 | 15300 | 598 | 0.5 | 0.07 |
| 6 | H$_2$O | 80 | 573 | 14300 | 590 | 8 | 2.0 |
| 7 | MeOH | 32.7 | -$^a$ | -$^a$ | -$^a$ | -$^a$ | -$^a$ |
| 8 | EtOH | 24.5 | 565 | 9500 | 591 | 8 | 2.0 |
| 9 | PentOH | 13.9 | -$^a$ | -$^a$ | -$^a$ | -$^a$ | -$^a$ |

Table S1. Optical properties of dioxa **1** in different solvents. Quantum yields relative to sulforhodamine 101 (EtOH, $\varphi_{fl}$ = 95%). $^a$ Due to limited solubility, values are not determined.

The most red-shifted fluorescence spectrum has been acquired in DMSO (598 nm) whereas the least one has been measured in DCM (592 nm). This could indicate the stabilization of the excited states by

polar solvents. DCM→ACN→DMSO for 592→595→598 nm respectively, difference of 170 cm$^{-1}$. Considering those three solvents, the solvatochromism is less pronounced for **1** compared to **2** and to a larger extend to **3**.

Fluorescence in water does not follow the same bathochromic trend. However, in this case it is difficult to link the solvent polarity to the excited state stabilization. Fluorescence in H$_2$O is located at 590 nm and show a hypsochromic shift compared to emission spectrum in DMSO.
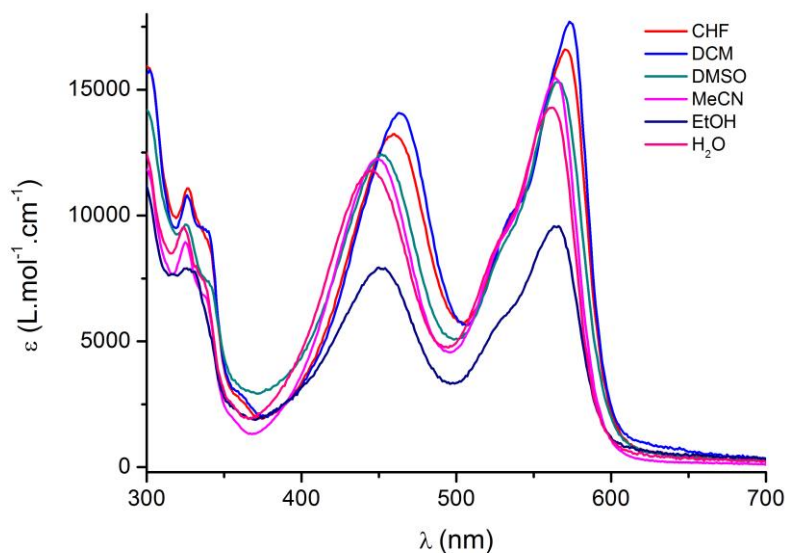


Figure S12. Absorption spectra of **1** in different solvents (C = 1.0 10$^{-5}$ M).
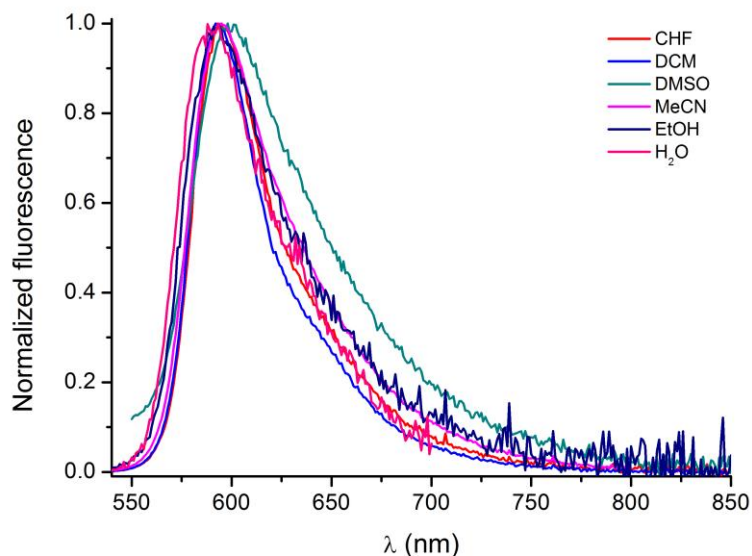


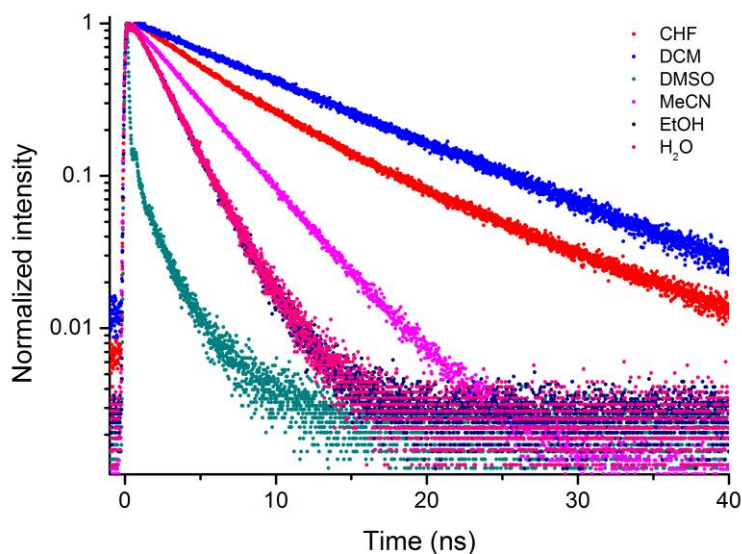Figure S13. Normalized fluorescence spectra of **1** in different solvents.

Figure S14. Intensity normalized fluorescence time profiles of **1** in different solvents.

## 2.3.2 Azaoxa [6]helicene 2

The optical properties of azaoxa **2** in 9 different solvents are gathered in Table S2.

| Entry | Solvent | $\varepsilon_r$ | $\lambda_{abs}$ (nm) | $\varepsilon$ (mol$^{-1}$.L.cm$^{-1}$) | $\lambda_{emm}$ (nm) | $\varphi_{fluo}$ (%) | $\tau$ (ns) |
|-------|---------|-----|------|------|------|------|------|
| 1 | CH$_3$CN | 37.5 | 562 | 10700 | 614 | 19 | 6.8 |
| 2 | CH$_2$Cl$_2$ | 9 | 574 | 11300 | 611 | 28 | 12.5 |
| 3 | CHCl$_3$ | 4.8 | 567 | 13050 | 617 | 14.5 | 7.8 |
| 4 | THF | 7.5 | 565 | 10900 | 612 | 10 | 5.8 |
| 5 | DMSO | 46.7 | 564 | 11400 | 622 | 7 | 4.0 |
| 6 | H$_2$O | 80 | 561 | 10200 | 610 | 7 | 4.0 |
| 7 | MeOH | 32.7 | 565 | 11000 | 613 | 10 | 5.5 |
| 8 | EtOH | 24.5 | 565 | 11300 | 616 | 11 | 6.0 |
| 9 | PentOH | 13.9 | 569 | 11500 | 616 | 12 | 6.5 |

Table S2. Optical properties of azaoxa **2** in different solvents. Quantum yields relative to sulforhodamine 101 (EtOH, $\varphi_{fl}$ = 95%).

Considering CH$_2$Cl$_2$ (entry 2), CH$_3$CN (entry 1) and DMSO (entry 5), a red shift of the fluorescence is observed in function of the solvents polarity. This spectral shift (11 nm) is less marked than for diaza **3** (16 nm) but more prominent than for **1** (6 nm). Viscosity seems to have no significant influence on fluorescence properties. For instance in DMSO and/or pentanol no noticeable increase of lifetimes nor fluorescence quantum yield is observable.
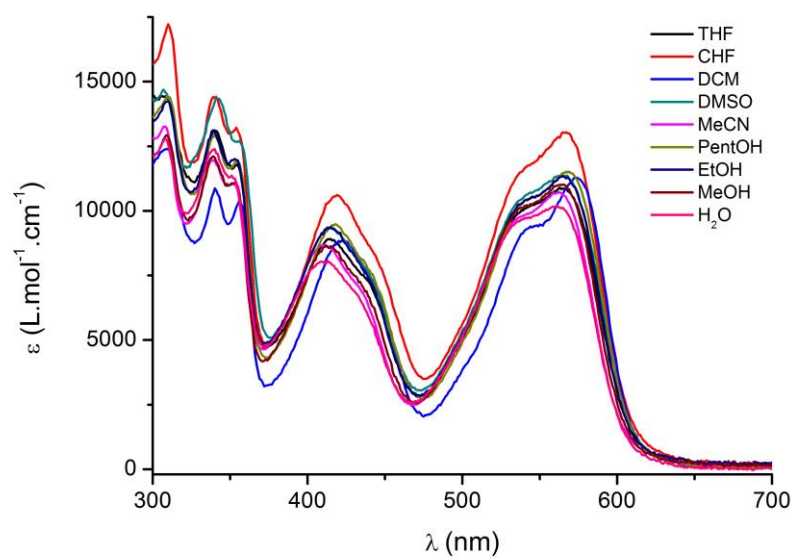
Figure S15. Absorption profile of azaoxa **2** in different solvents (C = 1.0 $10^{-5}$ M).
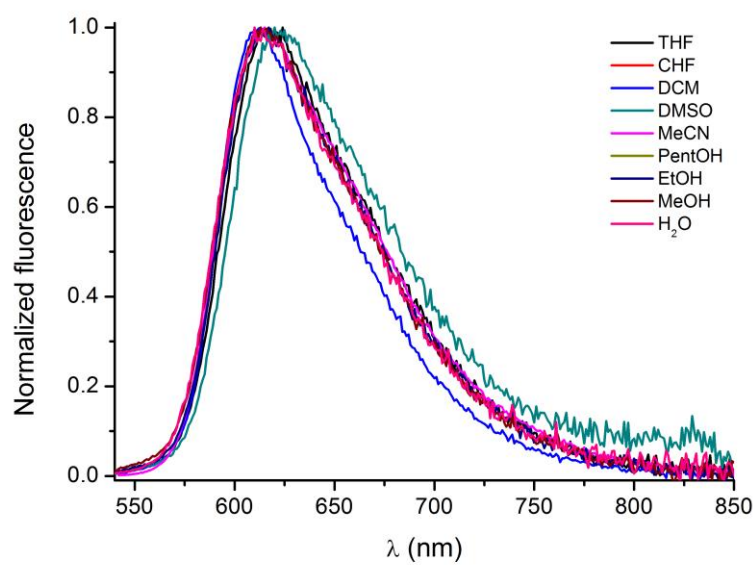


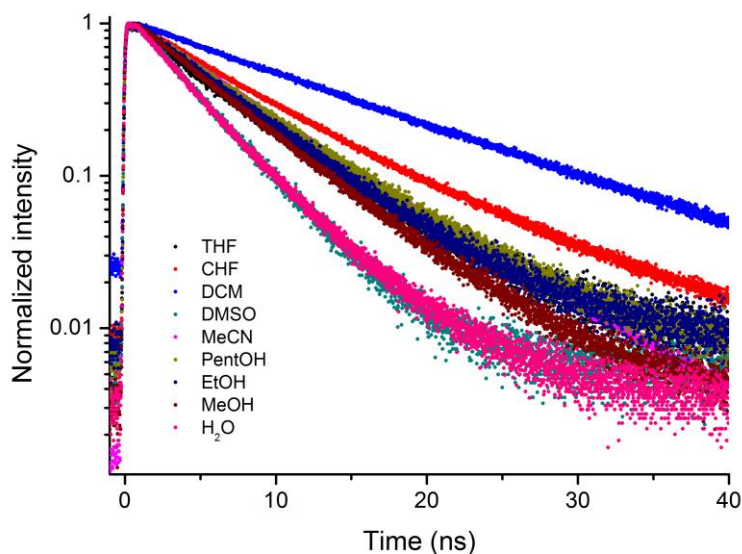Figure S16. Normalized fluorescence of **2** in different solvents.

Figure S17. Intensity normalized fluorescence time profiles of **2** in different solvents.

### 2.3.3 Diaza [6]helicene 3

The optical properties of diaza **3** in different solvents are gathered in Table S3. The fluorescence of **3** is clearly dependent on solvent polarity: the more polar the solvent, the more red-shifted the emission. Indeed some polar solvent molecules in the immediate relaxed surrounding of the cation reorganize themselves around the excited-state dipolar moment of the fluorophore. This induces a stabilization of the excited-state leading to a red shift of the fluorescence. For example, in DMSO, which dielectric constant ($\varepsilon_r$) is 46.7; the maximum of emission is localized at 664 nm (entry 5). On the other hand, the maximum emission wavelength of **3** in a less polar solvent *i.e.* CHCl$_3$ ($\varepsilon_r$ = 4.81) is localized at 653 nm (entry 3). The fact that there is no red shift in water (the most polar solvent of the list) could be explained by the lower solubility leading to a lowering of the interaction and thus a lower stabilization of the excited state (entry 6). Finally, the fluorescence decays show that the more the solvent is polar the shortest is the decay.

| Entry | Solvent | $\varepsilon_r$ | $\lambda_{abs}$ (nm) | $\varepsilon$ (mol$^{-1}$.L.cm$^{-1}$) | $\lambda_{emm}$ (nm) | $\varphi_{fluo}$ (%) | $\tau$ (ns) |
|---|---|---|---|---|---|---|---|
| 1 | CH$_3$CN | 37.5 | 614 | 14700 | 658 | 20.1 | 9.8 |
| 2 | CH$_2$Cl$_2$ | 9 | 619 | 15900 | 648 | 28.4 | 15.6 |
| 3 | CHCl$_3$ | 4.8 | 620 | 10200 | 653 | 16.7 | 11.8 |
| 4 | THF | 7.5 | 628 | -[a] | 655 | -[a] | 9.8 |
| 5 | DMSO | 46.7 | 620 | 15900 | 664 | 10.3 | 6.6 |
| 6 | H$_2$O | 80 | 617 | 13500 | 654 | 9.1 | 5.1 |
| 7 | MeOH | 32.7 | 615 | 11400 | 655 | 12.2 | 8.2 |
| 8 | EtOH | 24.5 | 622 | -[a] | 651 | -[a] | 9.0 |
| 9 | PentOH | 13.9 | 623 | -[a] | 650 | -[a] | 9.6 |

Table S3. Optical properties of diaza **3** in different solvents. Quantum yields relative to oxazine 725 (EtOH, $\varphi_{fl}$ = 11%). [a] Due to limited solubility, values are not determined.
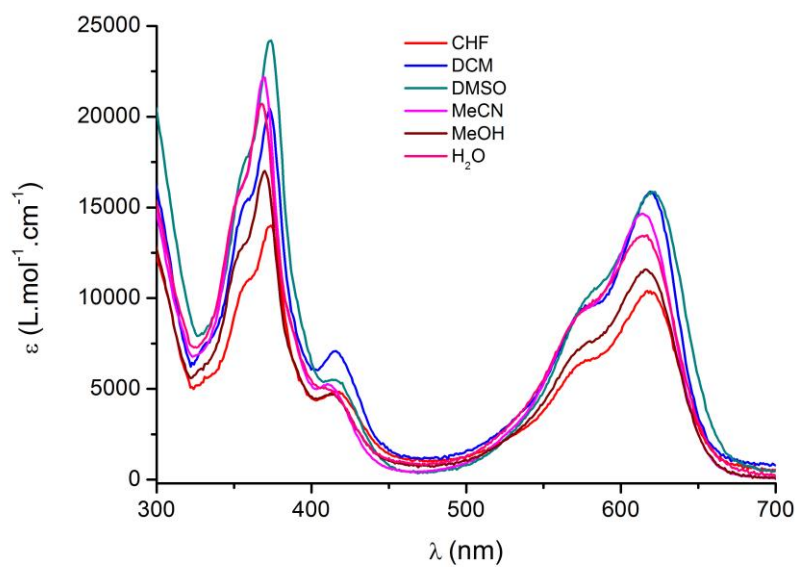
Figure S18. Absorption of diaza **3** in different solvents (C = 1.0 $10^{-5}$ M).
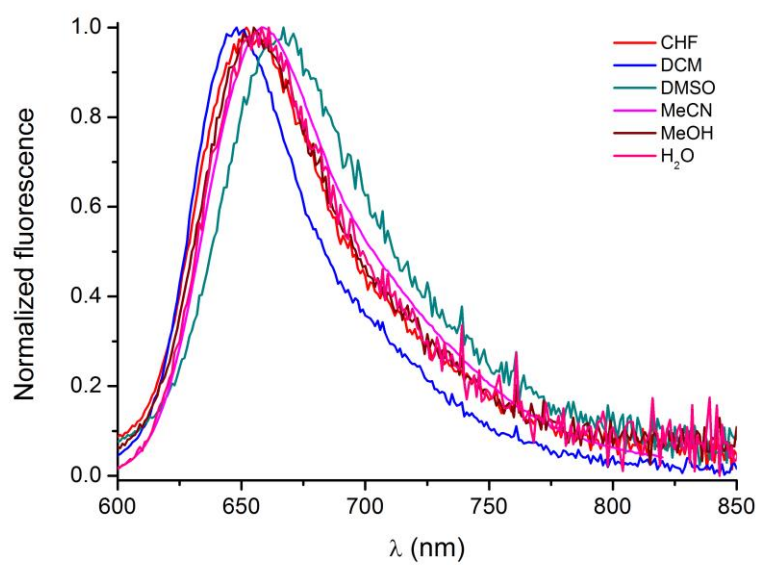


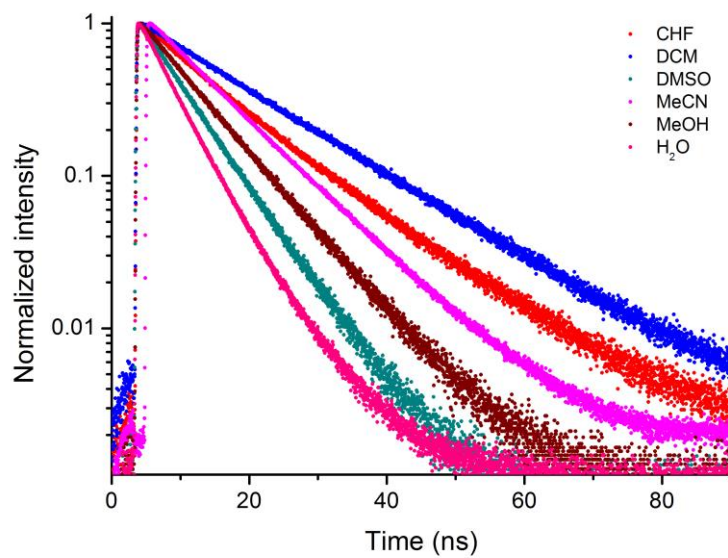Figure S19. Normalized fluorescence of **3** in different solvents.

Figure S20. Intensity normalized fluorescence time profiles of **3** in different solvents.
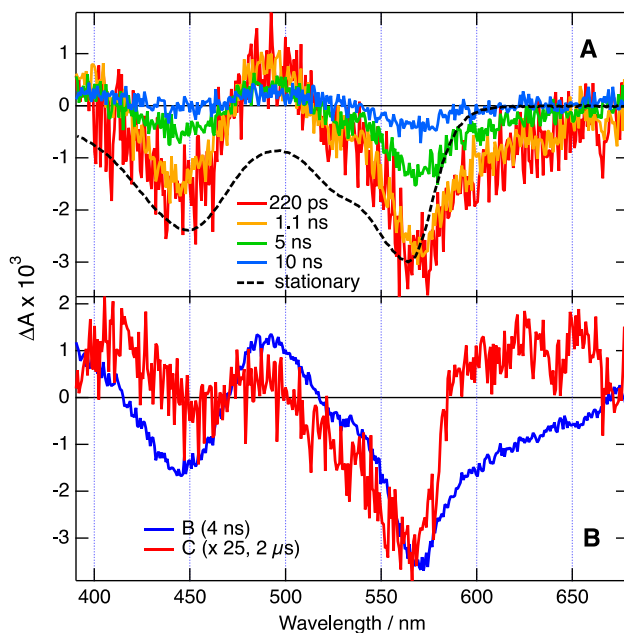
## 2.4 Transient absorption of compounds 1 – 3



Figure S21. A) Transient absorption spectra recorded at various time delays after 355 nm excitation of **1** in acetonitrile; B) species-associated difference spectra obtained from target analysis assuming an B → C → scheme.



Figure S22. A) Transient absorption spectra recorded at several time delays after 400 nm excitation of **2** in acetonitrile and inverted stationary absorption spectrum (dashed); B) species-associated difference absorption spectra obtained from global target analysis assuming an A → B → scheme.

Figure S23. A) Transient absorption spectra recorded at various time delays after 355 nm excitation of **2** in acetonitrile; B) species-associated difference spectra obtained from target analysis assuming an B → C → scheme.
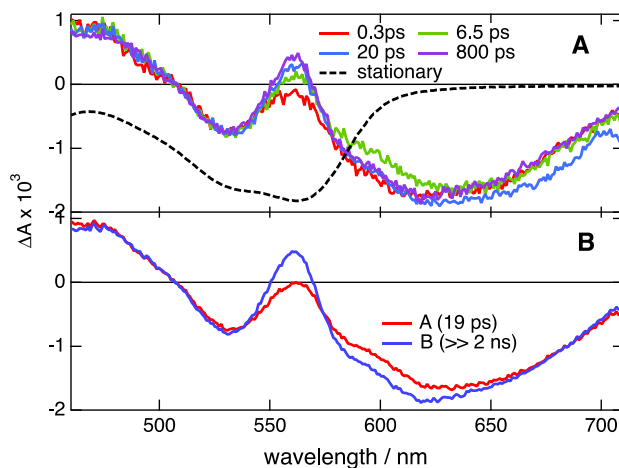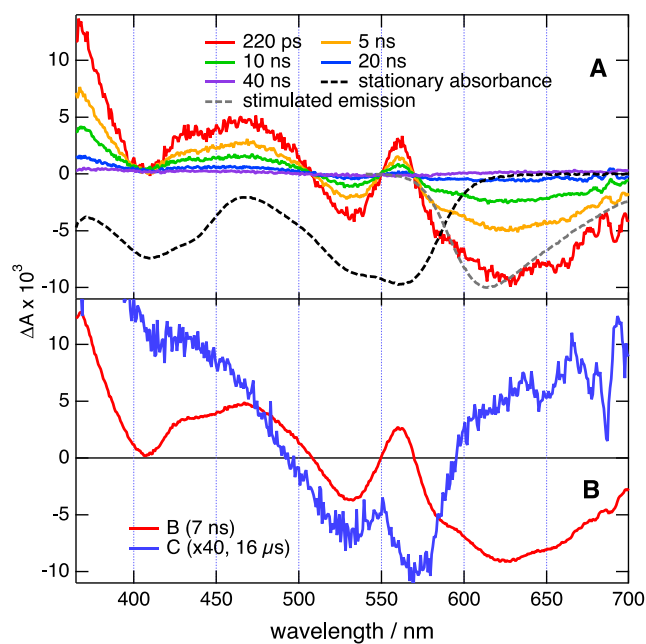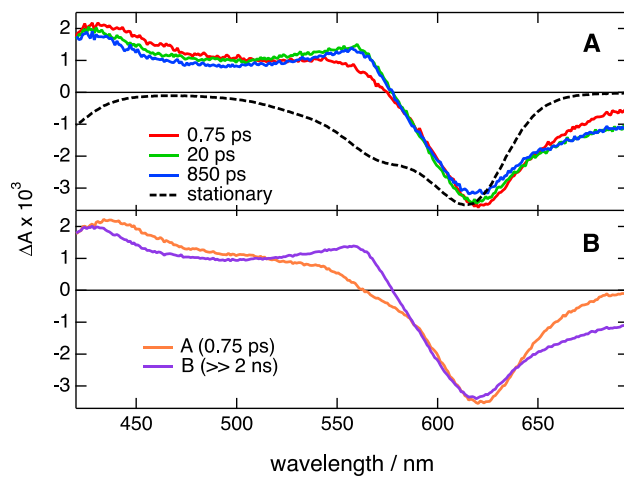


Figure S24. A) Transient absorption spectra recorded at several time delays after 400 nm excitation of **3** in acetonitrile and inverted stationary absorption spectrum (dashed); B) species-associated difference absorption spectra obtained from global target analysis assuming an A → B → scheme.

## 2.5 Circularly polarized luminescence (CPL) of compounds 1, 2 and 3

The circularly polarized luminescence (CPL) and total luminescence spectra were recorded on an instrument described previously,[11] operating in a differential photon-counting mode. The light source for excitation was a continuous wave 1000 W xenon arc lamp from a Spex Fluorolog-2 spectrofluorimeter, equipped with excitation and emission monochromators with dispersion of 4 nm/mm (SPEX, 1681B). To prevent artifacts associated with the presence of linear polarization in the emission,[12] a high quality linear polarizer was placed in the sample compartment, and aligned so that the excitation beam was linearly polarized in the direction of emission detection (z-axis). The key feature of this geometry is that it ensures that the molecules that have been excited and that are subsequently emitting are isotropically distributed in the plane (x,y) perpendicular to the direction of emission detection. The optical system detection consisted of a focusing lens, long pass filter, and 0.22 m monochromator. The emitted light was detected by a cooled EMI-9558B photomultiplier tube operating in photo-counting mode. All measurements were performed with quartz cuvettes with a path length of 1.0 cm.

# 3 Synthesis

## 3.1 General remarks

Microwave (MW) assisted reactions were performed in a Biotage Initiator® Microwave Synthesizer. Rf were measured on TLC Silica gel 60 F254 plates purchased from Merck.

Chromatographic separations were performed on a Teledyne Isco CombiFlash Rf200® apparatus using 4 g silica cartridges.

NMR spectra were recorded on Brucker AMX-500 at room temperature. $^1$H NMR: chemical shifts are given in ppm relative to Me$_4$Si with solvent resonances used as internal standards (5.32 ppm for CD$_2$Cl$_2$). Data were reported as follows: chemical shift ($\delta$) in ppm on the $\delta$ scale, multiplicity (s = singulet, brs = broad singulet, d = doublet, t = triplet, dd = doublet of doublet, h = hexuplet and m = multiplet), coupling constant (Hz) and integration. $^{13}$C NMR: chemicals shifts were given in ppm relative to Me$_4$Si with solvent resonances used as internal standards (53.84 ppm for CD$_2$Cl$_2$). IR spectra were recorded with a Perkin-Elmer 1650. FT-IR spectrometer using a diamond ATR Golden Gate sampling. Melting points (M.P.) were measured in open capillary tubes with a Buchi B-550 melting points apparatus and are uncorrected. Electrospray mass spectra were obtained on a Finnigan SSQ 7000 spectrometer by the Department of Mass Spectroscopy of the University of Geneva. UV/Visible spectra were obtained using a JASCO-650 spectrometer.

All compounds except **9**, **12** and **14** were prepared according to F. Torricelli, J. Bosson, C. Besnard, M. Chekini, T. Bürgi and J. Lacour, *Angew. Chem. Int. Ed.* **2013**, *52*, 1796-1800.

## 3.2 Previously reported and novel compounds

Helicenes **1**, **2**, **3** were synthesized from a common precursor obtained in 5 chemical steps following a reported procedure.[13] New compounds **9**, **12** and **14** are indicated in blue in the following schemes.

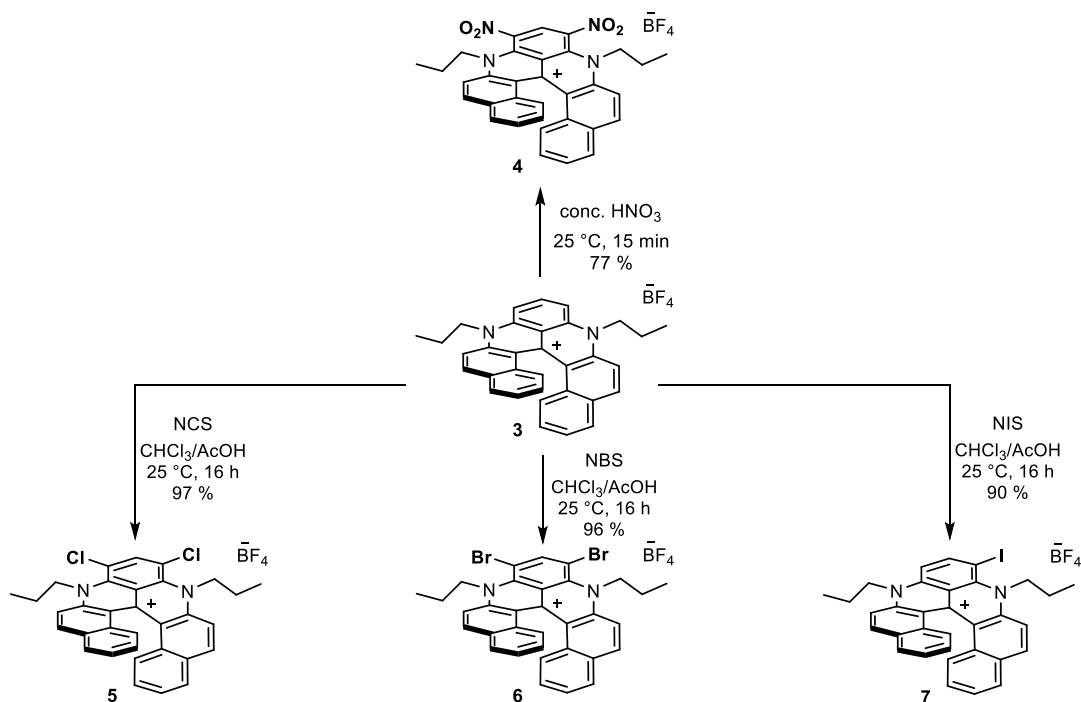### 3.2.1 Synthesis of the common precursor to 1 - 3



**Combined yield: 59% (15 g) on a 10 g scale**
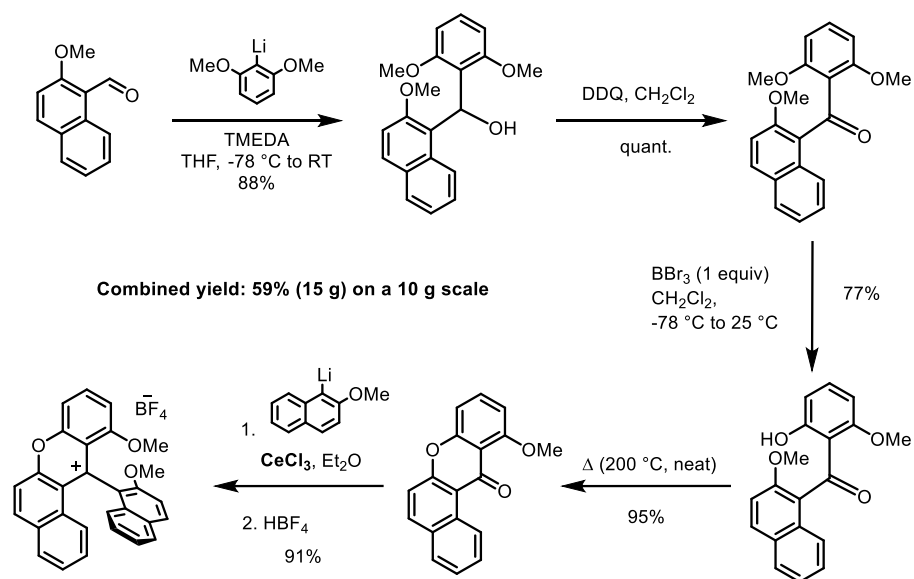
Scheme S1. Synthesis of the common precursor to **1** - **3**.

### 3.2.2 Synthesis of core structures 1 to 3
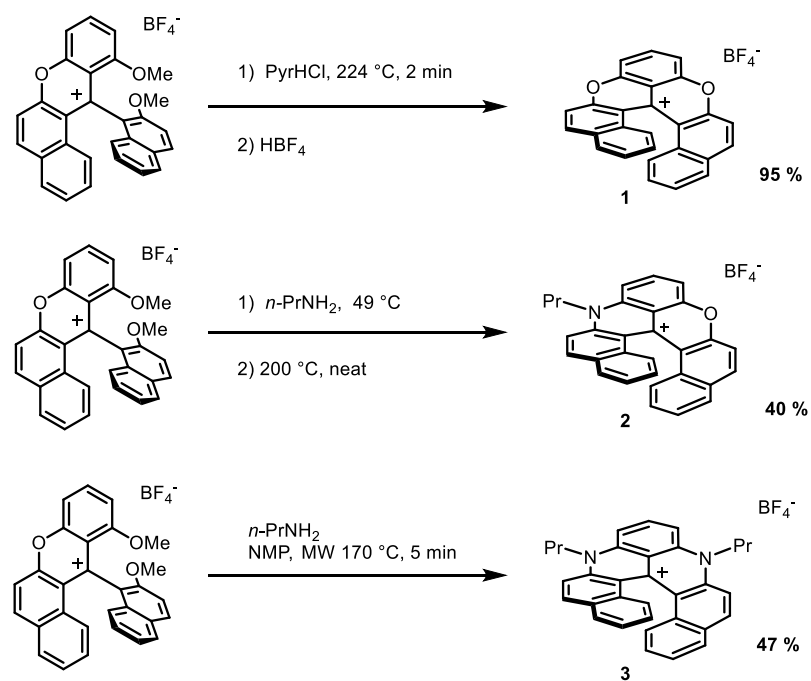


Scheme S2. Synthesis of core structures **1** - **3**.

### 3.2.3 Preparation of Dinitro derivative 4 and of Halogeno derivatives 5-7



Scheme S3. Preparation of Dinitro derivative **4** and of Halogeno derivatives **5** - **7**. NCS = *N*-chlorosuccinimide, NBS = *N*-bromosuccinimide, NIS = *N*-iodosuccinimide

### 3.2.4 Access to compounds 8 – 10 through palladium-catalyzed cross-coupling reactions
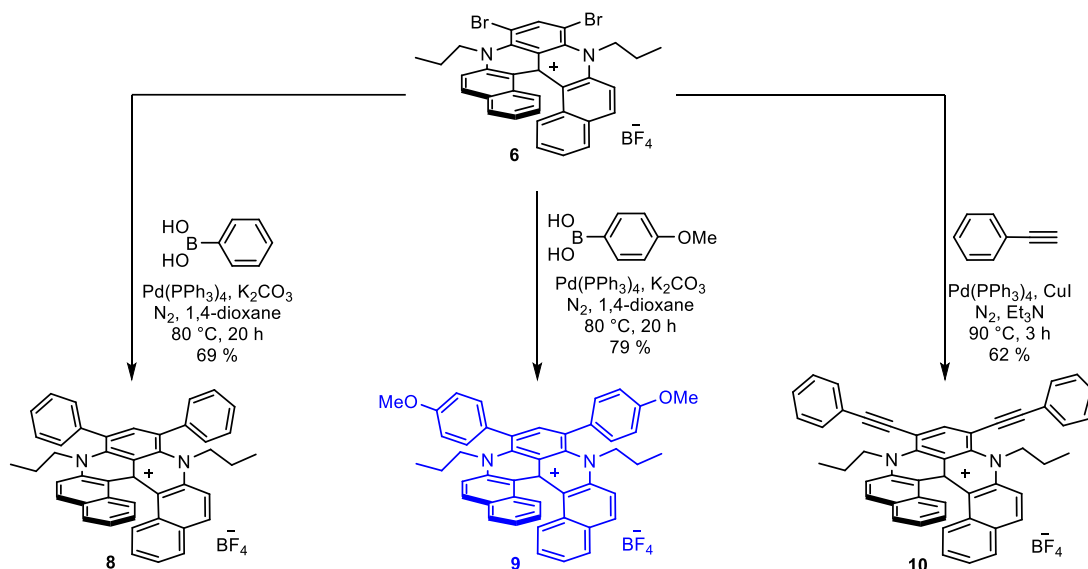


Scheme S4. Preparation of compounds **8** - **10**.

### 3.2.5 Preparation of amino derivatives 11 and 12
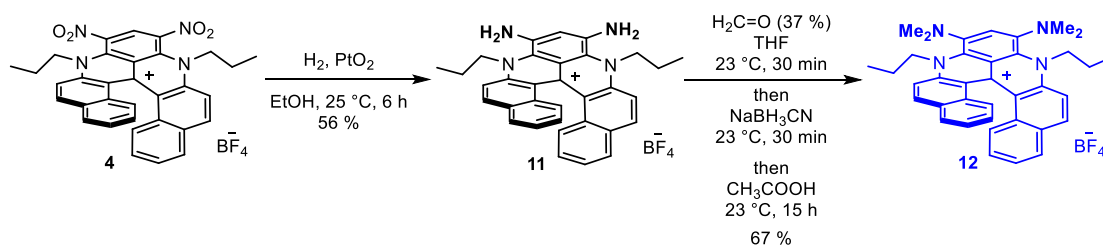


Scheme S5. Preparation of compounds **11** and **12**.

### 3.2.6 Preparation of compounds 13 to 15



Scheme S6. Preparation of compounds **13** - **15**.

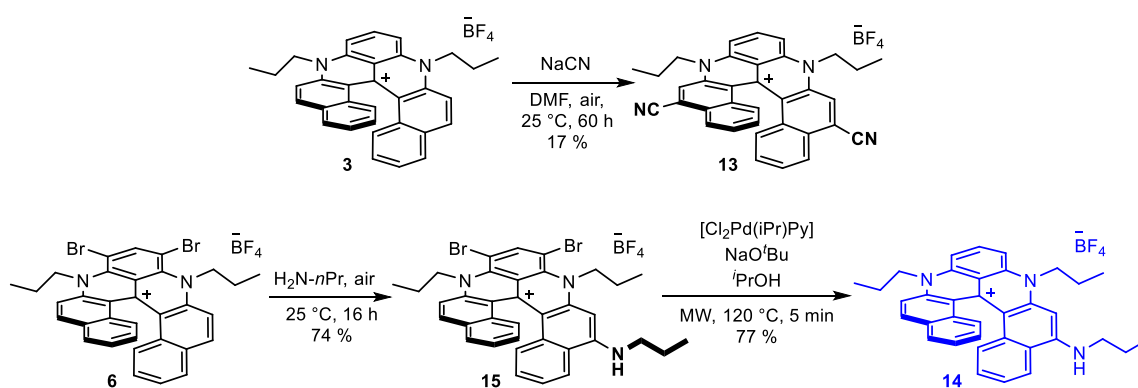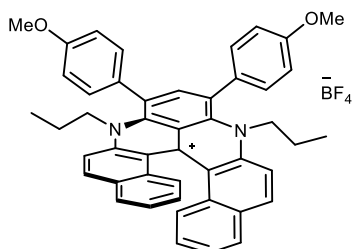### 3.3 Details of the synthesis of compounds 9, 12 and 14

#### 3.3.1 8,10-bis(4-methoxyphenyl)-7,11-dipropyl-7,11-dihydro-17cH-benzo[a]benzo[5,6]quinolino[2,3,4-kl]acridin-17c-ylium tetrafluoroborate 9

In a Schlenk tube under nitrogen atmosphere, $Pd(PPh_3)_4$ (3.6 mg, 0.003 mmol, 0.1 equiv.), potassium carbonate (16.2 mg, 0.12 mmol, 4 equiv.) and (4-methoxyphenyl) boronic acid (21.5 mg, 0.14 mmol, 5 equiv.) were added to a solution of **6** (20.0 mg, 0.0286 mmol, 1 equiv.) in 2 mL of dry 1,4-dioxane The resulting solution was stirred for 16 hours at 80 °C. After completion of the reaction monitored by TLC), the reaction mixture was allowed to get back to room temperature.

The reaction mixture was diluted with dichloromethane (5 mL) and washed three times with a 1 M aq. $HBF_4$ solution. The organic layer was dried over $Na_2SO_4$, filtered and evaporated. The residue was dissolved in a minimum amount of $CH_2Cl_2$ and $Et_2O$ was added, leading to the precipitation of the title compound, which was separated from the mother liquor by centrifugation.

The residue was then purified by flash chromatography (CombiFlash Rf200®, 4 g silica cartridge, $CH_2Cl_2$ / MeOH, from 100:00 to 95:05 over 50 min). The residue was precipitated ($CH_2Cl_2$ / $Et_2O$) and dried overnight under vacuum. 17 mg of title compound were obtained as a green solid (0.0225 mmol, Y = 79 %).

**M.P**. = 238 °C. **R***f* = 0.17 ($CH_2Cl_2$/MeOH 95:05). **$^1$H-NMR (500 MHz, $CD_2Cl_2$)**: δ 8.36 (d, *J* = 9,3 Hz, 2H), 8.20 (s, 1H), 7.92 (dd, *J* = 7.9 Hz, 1.6 Hz, 4H), 7.52 − 7.54 (m, 4H), 7.42 (t, *J* = 8.2 Hz, 2H), 7.15 (m, 6H), 6.94 (t, *J* = 8.3 Hz 2H), 4,38 − 4.44 (m, 2H), 4,04 − 4.10 (m, 2H), 3.93 (s, 6H), 1.62 - 1.66 (m, 4H), 0.43 (t, *J* = 6.9 Hz, 6H). **$^{13}$C-NMR (126 MHz, $CD_2Cl_2$)**: δ 160.14 (C), 144.69 (C), 140.54 (CH), 140.43 (C), 138.55(C), 135.48 (C), 131.43 (C), 129.52 (C), 128.98 (CH), 128.86 (CH), 128.34 (CH), 128.30 (CH), 127.71 (C), 126.30 (CH), 125.15 (C), 122.70 (CH), 120.20 (C), 116.88(CH), 115.35 (CH), 55.62 (OCH3), 55.51 (CH2), 22.63 (CH2), 10.51 (CH3). **$^{19}$F NMR (282 MHz, $CD_2Cl_2$)**: δ -152.57, -152.63. **IR (neat, cm$^{-1}$)**: λ 2961, 2928, 1605, 1580, 1548, 1515, 1472, 1285, 1250, 1214, 1179, 1057, 1030, 882, 827, 782, 751. **HRMS (ESI)** calc.: 665.3162; found: 665.3160.

#### 3.3.2 8,10-bis(dimethylamino)-7,11-dipropyl-7,11-dihydro-17cH-benzo[a]benzo[5,6]quinolino[2,3,4-kl]acridin-17c-ylium tetrafluoroborate 12
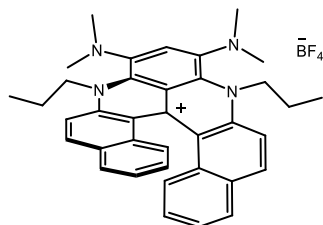
A 25 mL round bottom flask equipped with a stirring bar was charged with **11** (29 mg, 0.05 mmol), followed by THF (5 mL). After dissolution, formaldehyde (37 % wt in $H_2O$, 89 μL, 1.20 mmol, 24 equiv.) was added and the reaction mixture was stirred at 23 °C for 30 min. After this time, $NaBH_3CN$ (38 mg, 060 mmol, 12 equiv.) was added in one portion and the resulting reaction mixture was stirred for 30 additional minutes. After this time, acetic acid (2 mL) was added to the reaction mixture which was stirred for 15 hours.

After this time, aq. NaOH (10 % wt) was added dropwise to the reaction mixture, until a neutral pH was reached. This mixture was diluted with dichloromethane and washed three times with a 1 M aq. $HBF_4$ solution. The organic layer was dried over $Na_2SO_4$, filtered and evaporated. The residue was dissolved in a minimum amount of $CH_2Cl_2$ and a 1:1 pentane / $Et_2O$ mixture was added, leading to the precipitation of the title compound, which was separated from the mother liquor by centrifugation. This was repeated 3 times.

The residue was then purified by flash chromatography (CombiFlash Rf200®, 4 g silica cartridge, CH$_2$Cl$_2$ / MeOH, from 100:00 to 97:03 over 50 min). Finally, the residue was dissolved with CH$_2$Cl$_2$ and washed once with a 1 M aq. HBF$_4$ solution. The organic layer was dried over Na$_2$SO$_4$, filtered and evaporated. The residue was precipitated (CH$_2$Cl$_2$ / 1:1 pentane/Et$_2$O) and dried overnight under vacuum. 21 mg of title compound were obtained as a green solid (0.0335 mmol, Y = 67 %).

**M.P.** = 197 °C. **R***f* = 0.65 (CH$_2$Cl$_2$/MeOH 95:05). **$^1$H NMR (500 MHz, CD$_2$Cl$_2$)**: δ 8.28 (d, *J* = 10.0 Hz, 2H), 7.98 (d, *J* = 9.4 Hz, 2H), 7.84 (d, *J* = 7.8 Hz,, 2H), 7.46 (s, 1H), 7.33 (ddd, *J* = 8.0, 7.0, 1.1 Hz, 2H), 7.00 (dq, *J* = 8.4, 0.8 Hz, 2H), 6.84 (ddd, *J* = 8.5, 7.0, 1.4 Hz, 2H), 5.38 (dt, *J* = 14.6, 7.4 Hz, 2H), 4.71 (ddd, *J* = 13.8, 7.8, 5.6 Hz, 2H), 3.32 – 2.56 (m, 12H), 1.68 – 1.49 (m, 7H – overlapped with water), 0.57 (t, *J* = 7.4 Hz, 6H). **$^{13}$C NMR (125 MHz, CD$_2$Cl$_2$)**: δ 146.7 (C), 143.0 (C), 140.2 (C), 138.4 (CH), 129.8 (C), 129.3 (C), 129.1 (CH), 128.2 (CH), 127.6 (CH), 127.3 (C), 124.0 (C), 123.1 (CH), 120.4 (C), 117.1 (CH), 114.4 (CH), 50.0 (CH$_2$), 22.9 (CH$_2$), 11.4 (CH$_3$). **$^{19}$F NMR (282 MHz, CD$_2$Cl$_2$)**: δ -152.62, -152.67. **IR (neat, cm$^{-1}$)**: λ 2960, 2872, 2836, 2796, 1599, 1577, 1544, 1517, 1478, 1456, 1381, 1356, 1307, 1261, 1213, 1178, 1159, 1049, 979, 914, 879, 819, 778, 731, 702, 651, 621. **HRMS (ESI)**: calc: 539.3169; found: 539.3168.

### 3.3.3   7,11-dipropyl-5-(propylamino)-7,11-dihydro-17cH-benzo[a]benzo[5,6]quinolino[2,3,4-kl]acridin-17c-ylium tetrafluoroborate 14
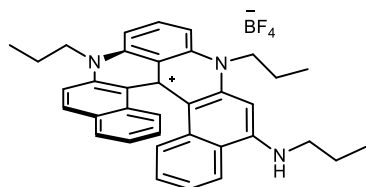


A 5 mL Microwave vial equipped with a stirring bar was charged with **15** (20 mg, 0.024 mmol), dichloro-1,3-di*iso*propylimidazolium-pyridine palladium ([Cl$_2$Pd(iPr)Py], 0.8 mg, 0.0012 mmol) and NaO*t*Bu (2.8 mg, 0.0288 mmol). The vial was sealed with a septum-cap and purged with N$_2$. *i*PrOH (0.5 mL) was added and the reaction mixture was stirred at 120 °C under microwave irradiation for 5 min.

After this time, the vial was unsealed, the reaction mixture was diluted with CH$_2$Cl$_2$ (10 mL) and washed twice with a 1 M aq. HBF$_4$ solution. The organic layer was dried over Na$_2$SO$_4$, filtered and evaporated. The residue was dissolved in a minimum amount of CH$_2$Cl$_2$ and Et$_2$O was added, leading to the precipitation of the title compound, which was separated from the mother liquor by centrifugation. This was repeated 3 times.

The residue was then purified by flash chromatography (CombiFlash Rf200®, 4 g silica cartridge, CH$_2$Cl$_2$ / MeOH, from 100:00 to 95:05 over 50 min). Finally, the residue was dissolved with CH$_2$Cl$_2$ and washed once with a 1 M aq. HBF$_4$ solution. The organic layer was dried over Na$_2$SO$_4$, filtered and evaporated. The residue was precipitated (CH$_2$Cl$_2$ / Et$_2$O) and dried overnight under vacuum. 11 mg of title compound were obtained as a dark purple solid (0.0184 mmol, Y = 77 %).

*Adapted from:* O. Navarro, H. Kaur, P. Mahjoor, S. P. Nolan *J. Org. Chem.* **2004**, *69*, 3173-3180.

**M.P.** = 214 °C (decomp). **R***f* = 0.55 (CH$_2$Cl$_2$/MeOH 95:05). **$^1$H NMR (500 MHz, CD$_2$Cl$_2$)**: δ 8.23 (d, *J* = 9.5 Hz, 1H), 8.03 (t, *J* = 8.0 Hz, 1H), 7.91 (ddd, *J* = 8.0, 1.0, 0.5 Hz, 1H), 7.83-7.79 (m, 2H), 7.48 (d, *J* = 8.5 Hz, 1H), 7.44 (d, *J* = 8.5 Hz, 1H), 7.35 (td, *J* = 7.0, 1.0 Hz, 1H), 7.29 (td, *J* = 7.0, 1.0 Hz, 1H), 7.21-7.19 m (2H), 6.86 (td, *J* = 7.0, 1.5 Hz, 1H), 6.77 (td, *J* = 7.0, 1.0 Hz, 1H), 6.49 (s, 1H), 6.36 (brt, *J* = 5.0 Hz, 1H), 4.69-4.60 (m, 2H), 4.53-4.46 (m, 1H), 4.43-4.36 (m, 1H), 3.65-3.60 (m, 2H), 2.23-2.12 (m, 4H), 6.36 (h, *J* = 7.5 Hz, 2H), 1.31 (1, *J* = 7.5 Hz, 3H), 1.27 (t, *J* = 7.5 Hz, 3H), 1.21 (t, *J* = 7.5 Hz, 3H). **$^{13}$C NMR (125 MHz, CD$_2$Cl$_2$)**: δ 153.1 (C), 146.2 (C), 142.0 (C), 139.2 (C), 138.5 (C), 138.3 (C), 137.4 (CH), 133.7 (CH), 131.3 (C), 129.7 (C), 129.6 (C), 128.8 (CH), 128.3 (CH), 128.0 (CH), 127.7 (CH), 126.7 (CH), 124.2 (CH), 123.0 (CH), 122.4 (C), 120.9 (CH), 119.8 (C), 115.3 (CH), 114.7 (C), 112.3 (C), 106.6 (CH), 106.5 (CH), 87.7 (CH), 51.4 (CH$_2$), 46.2 (CH$_2$), 28.3 (CH$_2$), 22.3 (CH$_2$), 20.8 (CH$_2$), 20.1 (CH$_2$), 11.9 (CH$_3$), 11.5 (CH$_3$), 11.3 (CH$_3$). **$^{19}$F NMR (282 MHz, CD$_2$Cl$_2$)**: δ -152.17, -152.22. **IR (neat, cm$^{-1}$)**: λ 3004, 2964, 2933, 2872, 1605, 1578, 1544, 1527, 1486, 1462, 1376, 1332, 1263, 1162, 1058, 811, 750. **HRMS (ESI)**: calc: 510.2904; found: 510.2899.

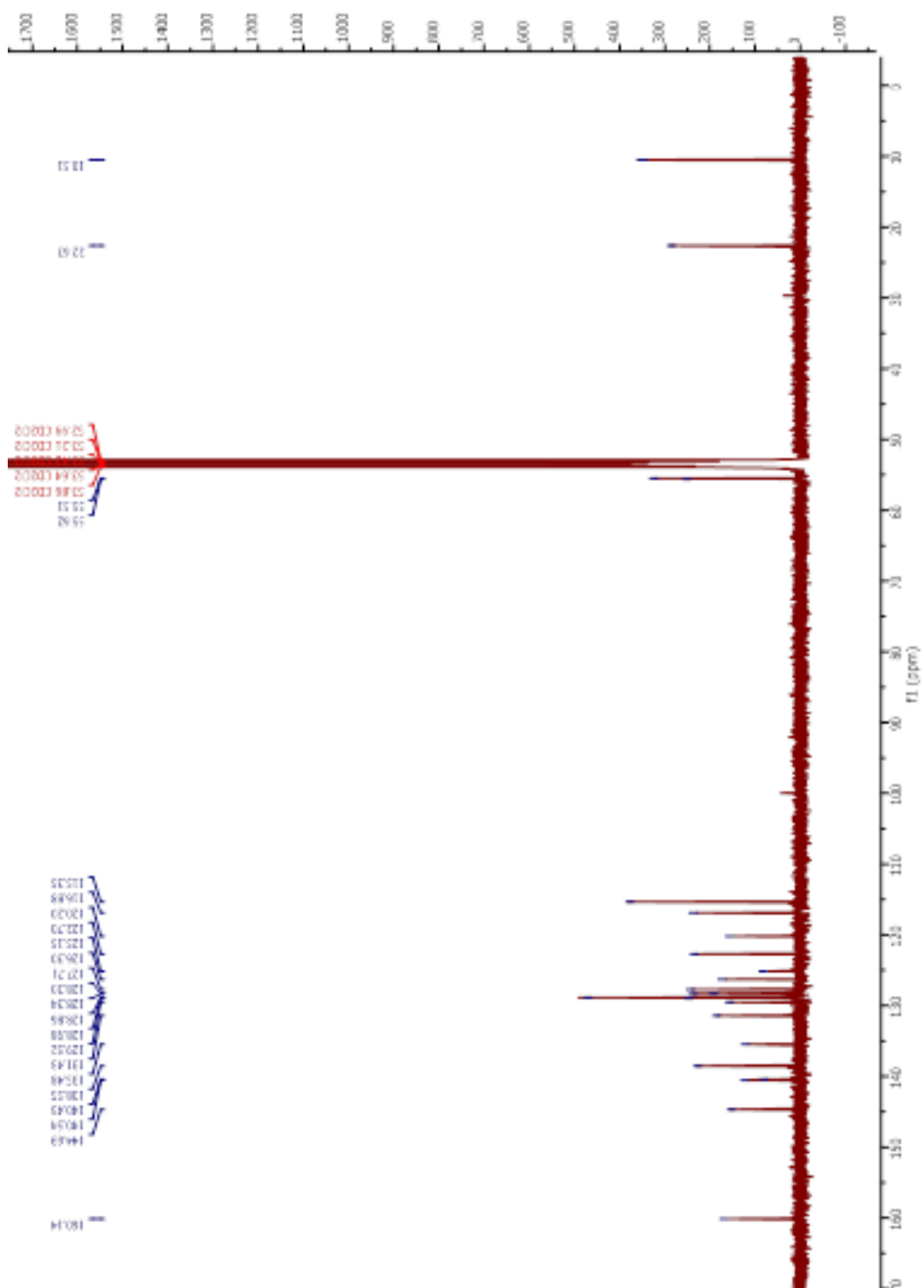## 3.4 Spectroscopic data for compounds 9, 12 and 14

### 3.4.1 8,10-bis(4-methoxyphenyl)-7,11-dipropyl-7,11-dihydro-17cH-benzo[a]benzo[5,6]quinolino[2,3,4-kl]acridin-17c-ylium tetrafluoroborate 9
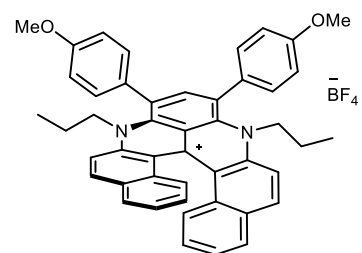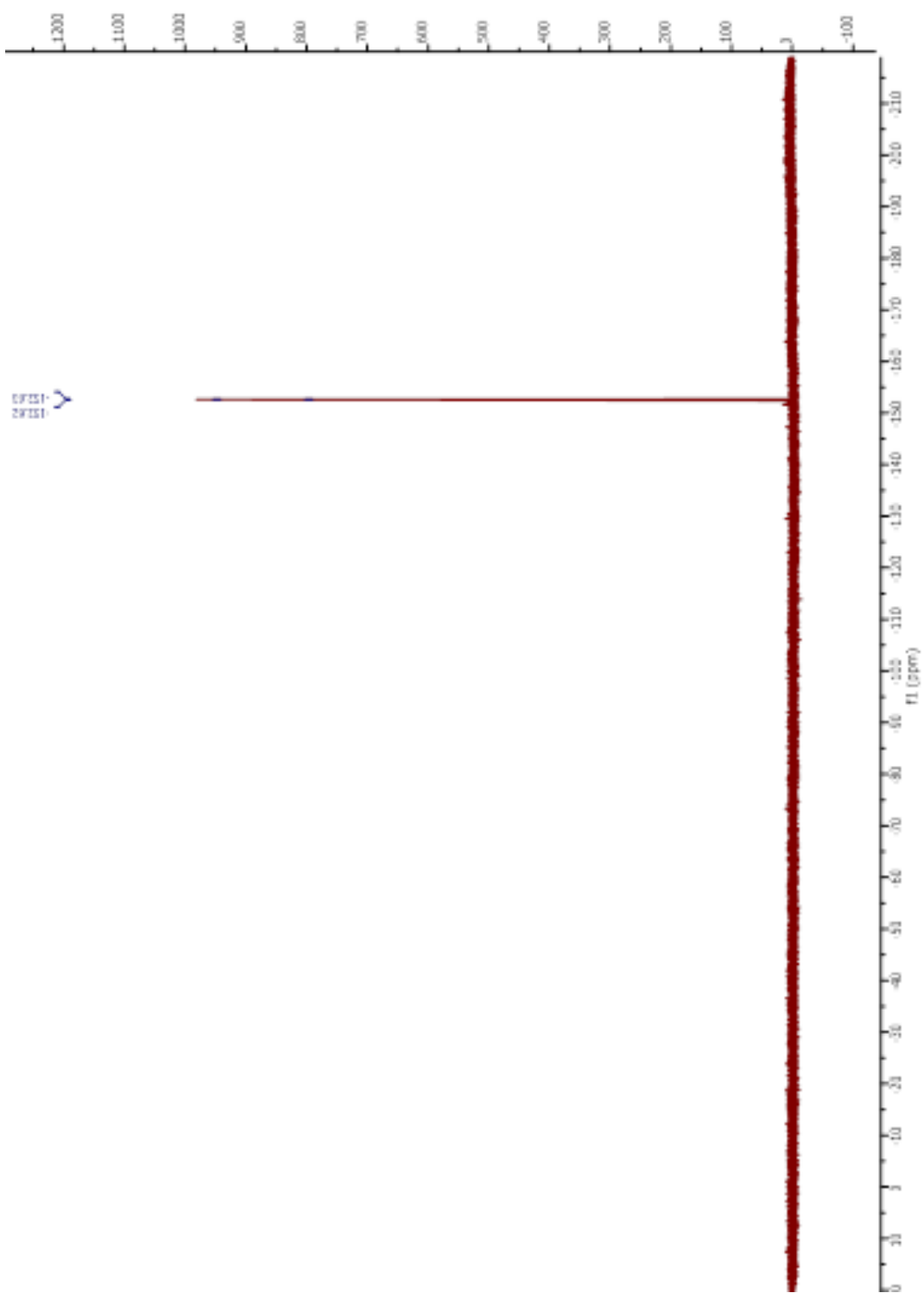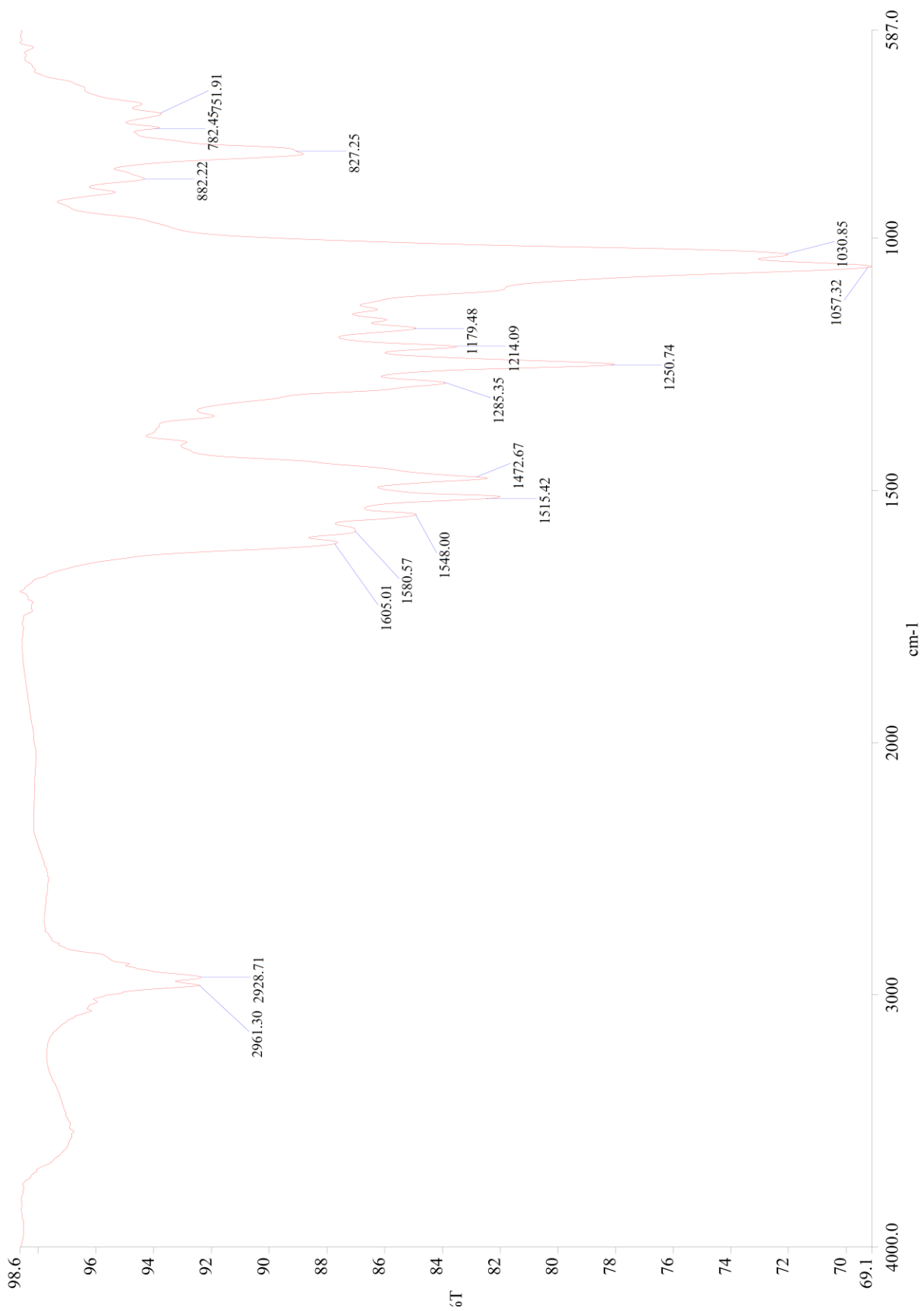
#### 3.4.1.1 $^1$H NMR (500 MHz, CD$_2$Cl$_2$)
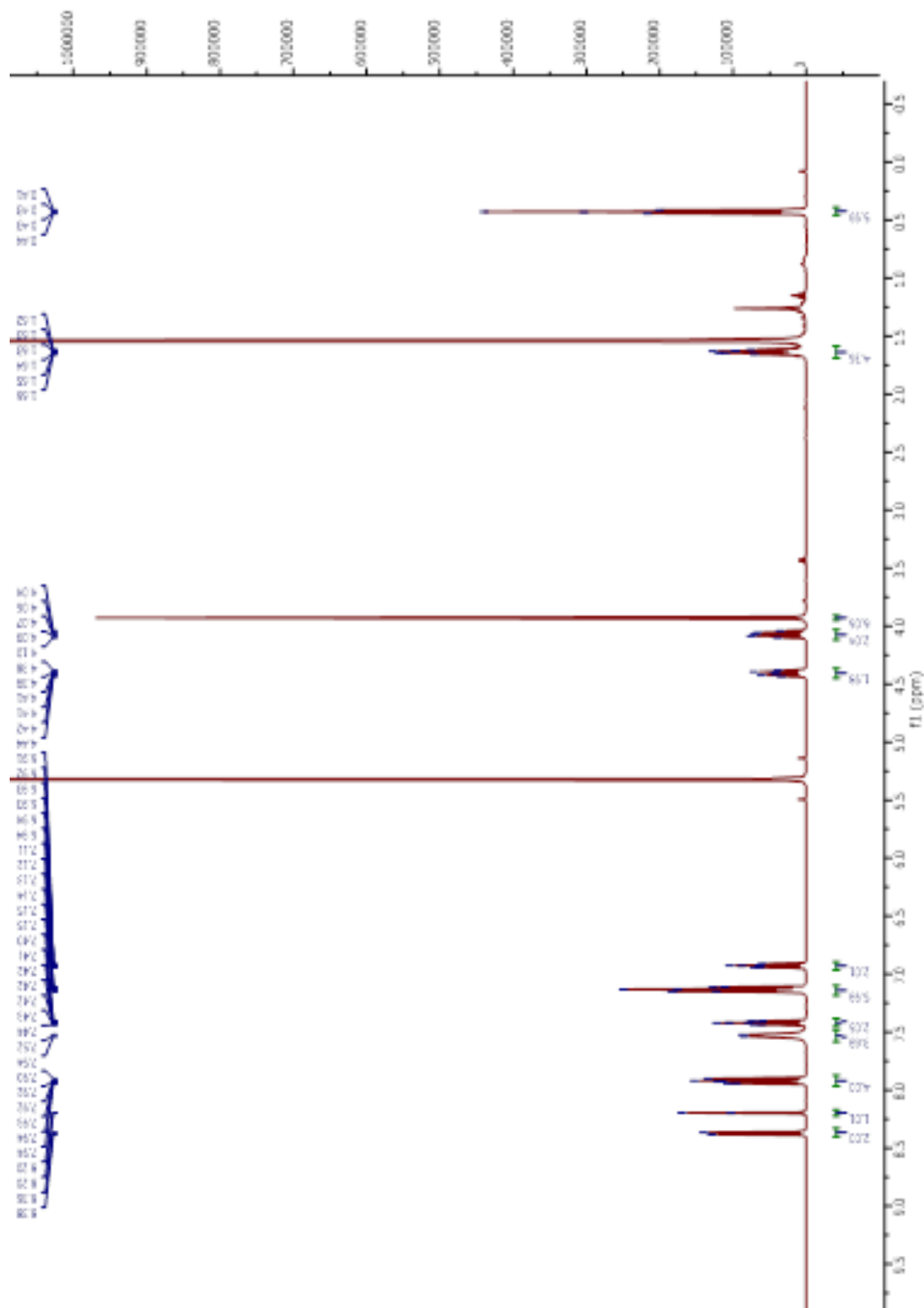
### 3.4.1.2 $^{13}$C NMR (125 MHz, CD$_2$Cl$_2$)

### 3.4.1.3  19F NMR (282 MHz, CD2Cl2)

### 3.4.1.4    IR (neat, cm-1)
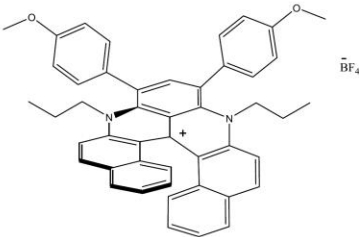
### 3.4.1.5   HRMS (ESI)

| | | | |
|---|---|---|---|
| Submitter: | LABRADOR | Date of reception: | 17/02/15 |
| Sample name: | GLDC235 | Date of certificate: | 23/02/15 |
| Sample number: | 7703 | Data filename: | SMS10GE-150223-ES-A002 |
| Operator: | Eliane Sandmeier | Instrument: | QSTAR Pulsar (AB/MDS Sciex) |
| Principal investigator: | Dr. Sophie Michalet | Ionisation mode: | ESI (positive mode) |

| Expected Formula | Observed $m/z$ [M]$^+$ | Expected $m/z$ (amu) | Accuracy (ppm) |
|---|---|---|---|
| $C_{47}H_{41}N_2O_2$ | 665.3160 | 665.3162 | -0.3 |



Chemical Formula: $C_{47}H_{41}BF_4N_2O_2$
Exact Mass: 752.32
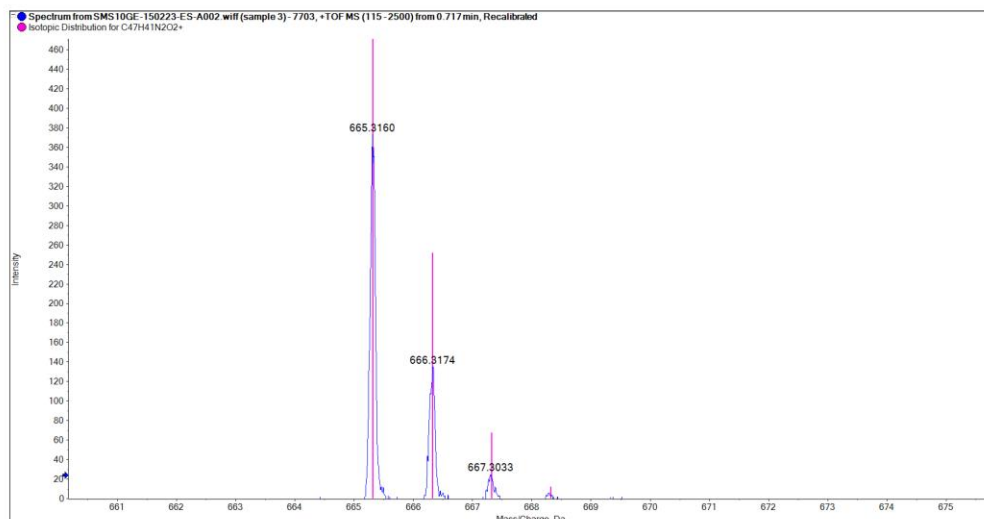
### 3.4.2 8,10-bis(dimethylamino)-7,11-dipropyl-7,11-dihydro-17cH-benzo[a]benzo[5,6]quinolino[2,3,4-kl]acridin-17c-ylium tetrafluoroborate 12
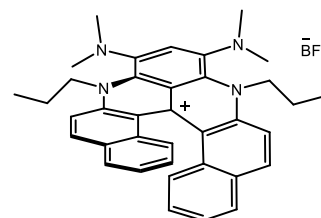
### 3.4.2.1 $^1$H NMR (500 MHz, CD$_2$Cl$_2$)

### 3.4.2.2    $^{13}$C NMR (125 MHz, CD$_2$Cl$_2$)

11.35

22.89

49.98

114.43
117.12
120.44
123.11
124.02
127.25
127.56
128.24
129.05
129.33
129.77

138.35
140.17
143.01
146.74
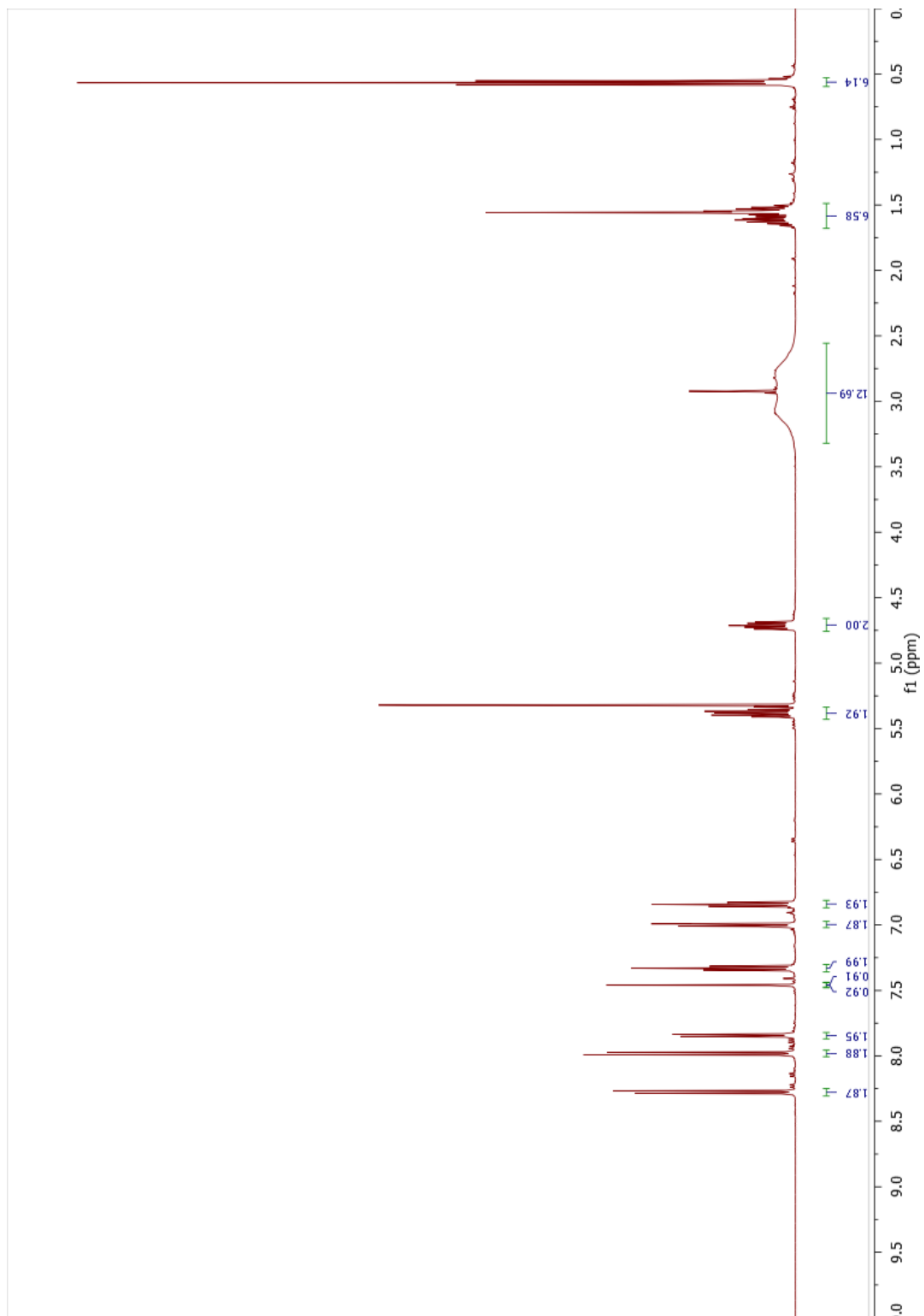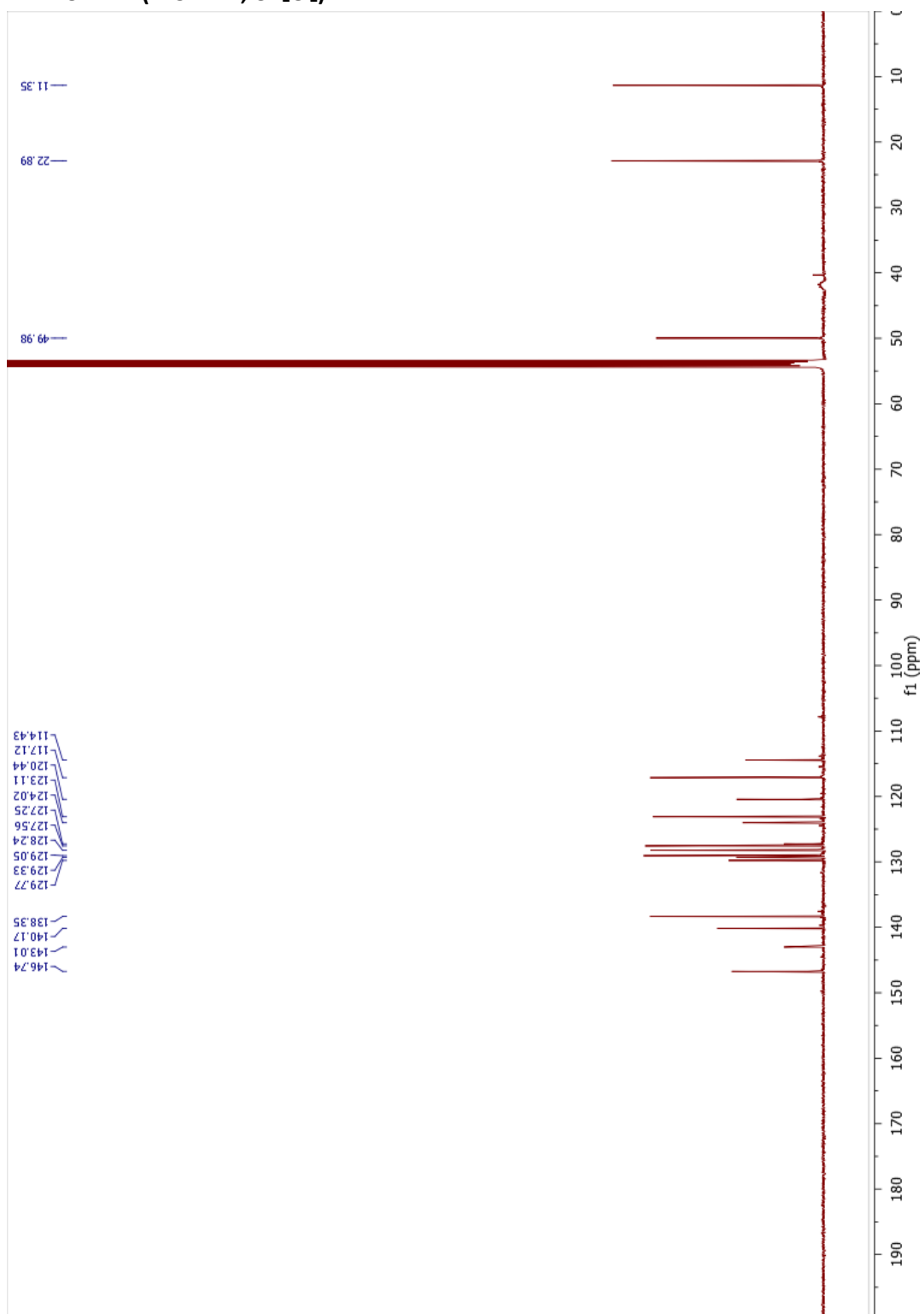
### 3.4.2.3 ¹⁹F NMR (282 MHz, CD₂Cl₂)

-152.67
-152.62

f1 (ppm)
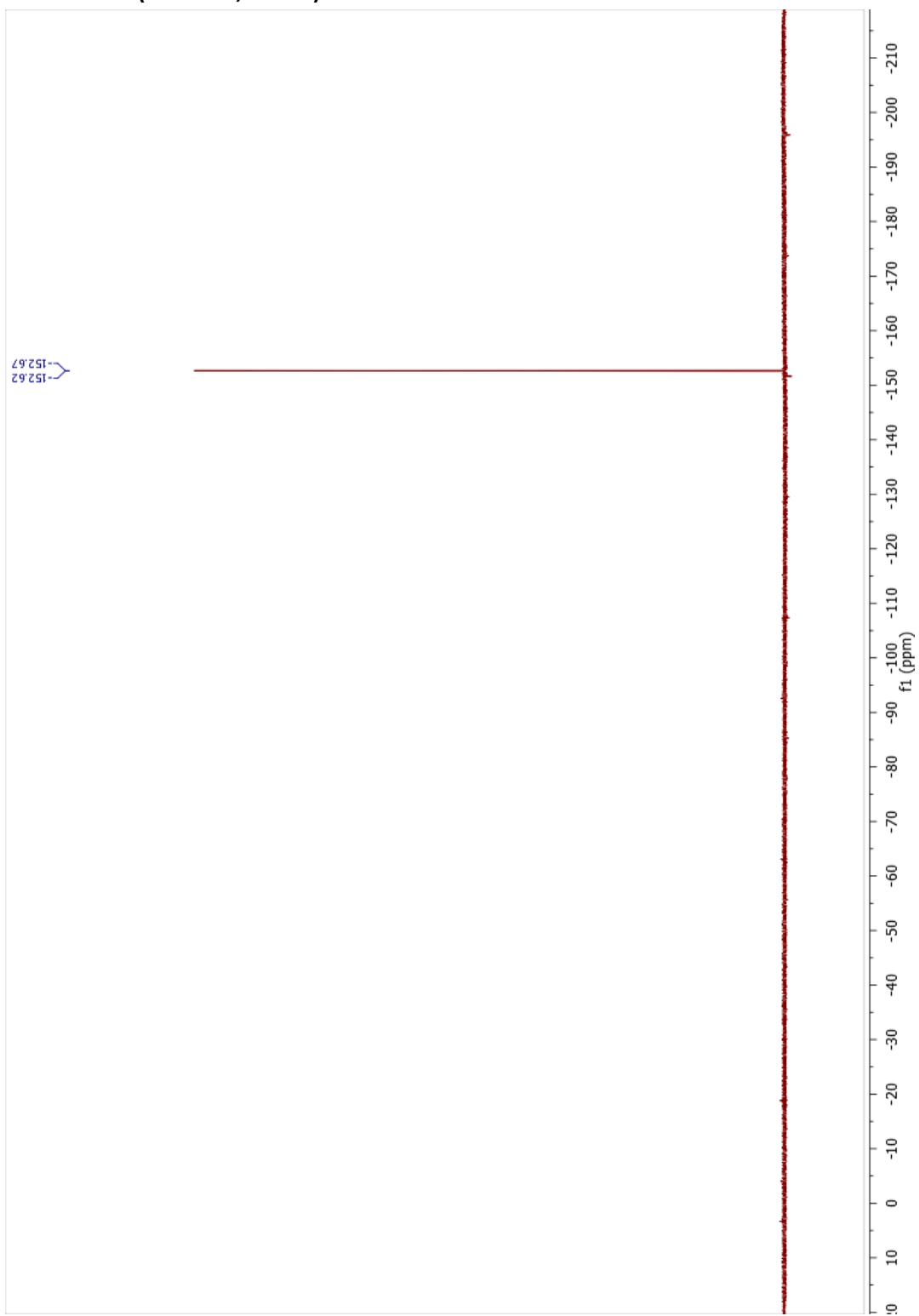
### 3.4.2.4 IR (neat, cm-1)
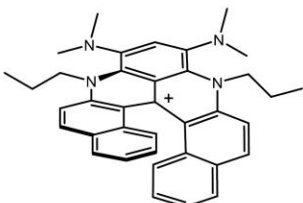
## 3.4.2.5    HRMS (ESI)

**UNIVERSITY OF GENEVA**

Faculty of Sciences

Sciences Mass Spectrometry

| | | | |
|---|---|---|---|
| Submitter: | BOSSON | Date of reception: | 23/02/15 |
| Sample name: | JB516 | Date of certificate: | 25/02/15 |
| Sample number: | 7710 | Data filename: | SMS10GE-150223-ES-A002 |
| Operator: | Eliane Sandmeier | Instrument: | QSTAR Pulsar (AB/MDS Sciex) |
| Principal investigator: | Dr. Sophie Michalet | Ionisation mode: | ESI (positive mode) |

| Expected Formula | Observed $m/z$ [M]$^+$ | Expected $m/z$ (amu) | Accuracy (ppm) |
|---|---|---|---|
| $C_{37}H_{39}N_4$ | 539.3168 | 539.3169 | -0.2 |



Chemical Formula: $C_{37}H_{39}N_4^+$
Molecular Weight: 539.7
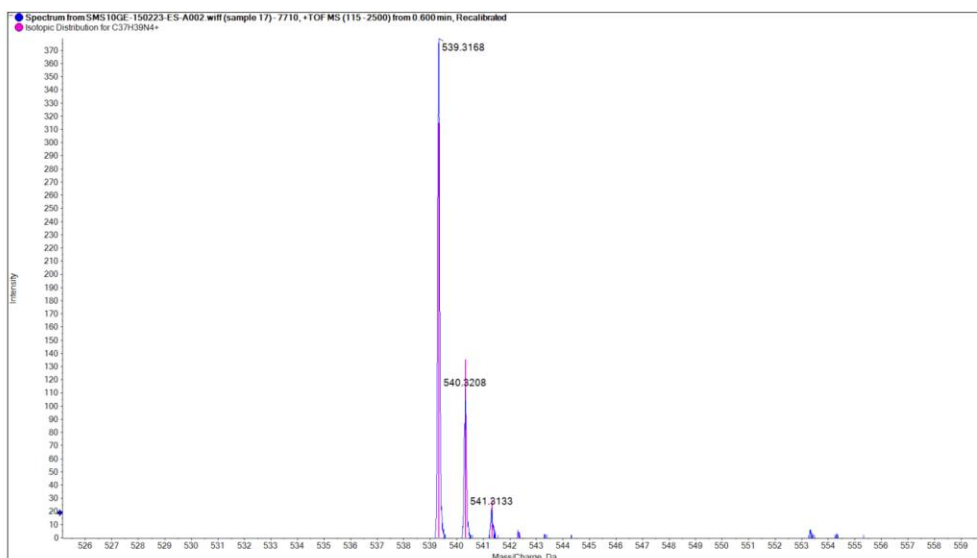
### 3.4.3 7,11-dipropyl-5-(propylamino)-7,11-dihydro-17cH-benzo[a]benzo[5,6]quinolino[2,3,4-kl]acridin-17c-ylium tetrafluoroborate 14



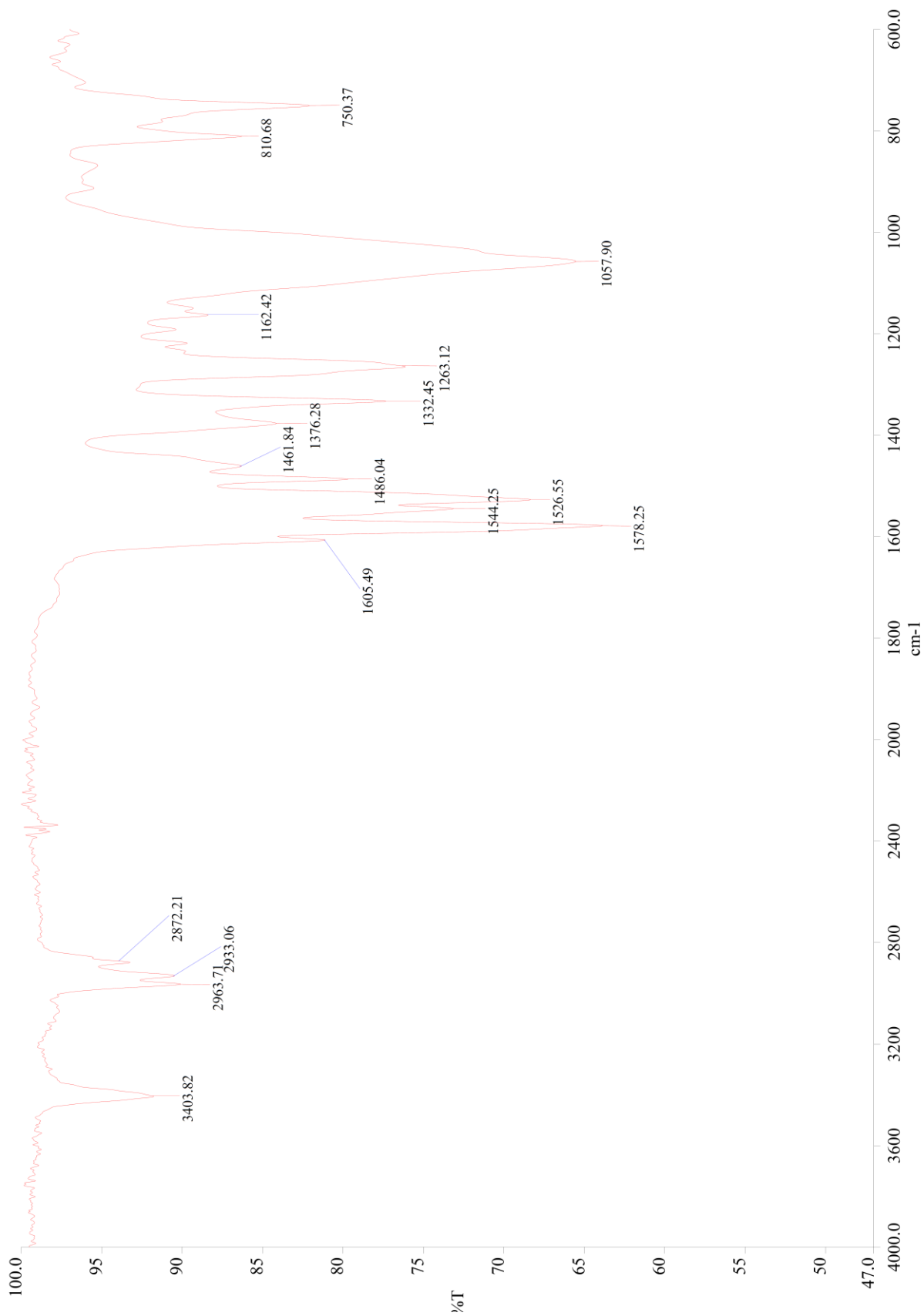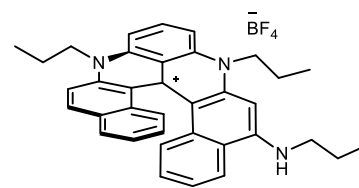#### 3.4.3.1   $^1$H NMR (500 MHz, CD$_2$Cl$_2$)

### 3.4.3.2    $^{13}C$ NMR (125 MHz, CD$_2$Cl$_2$)



Peak labels (ppm):
11.3, 11.5, 11.9
20.1, 20.8, 22.3
28.3
46.2
51.4
87.7
106.5, 106.6, 112.3, 114.7, 115.3, 119.8, 120.9, 122.4, 123.0, 124.2, 126.7, 127.7, 128.0, 128.3, 128.6, 129.6, 129.7, 131.3, 133.7, 137.4, 138.3, 138.5, 139.2, 142.0, 146.2, 153.1

f1 (ppm)
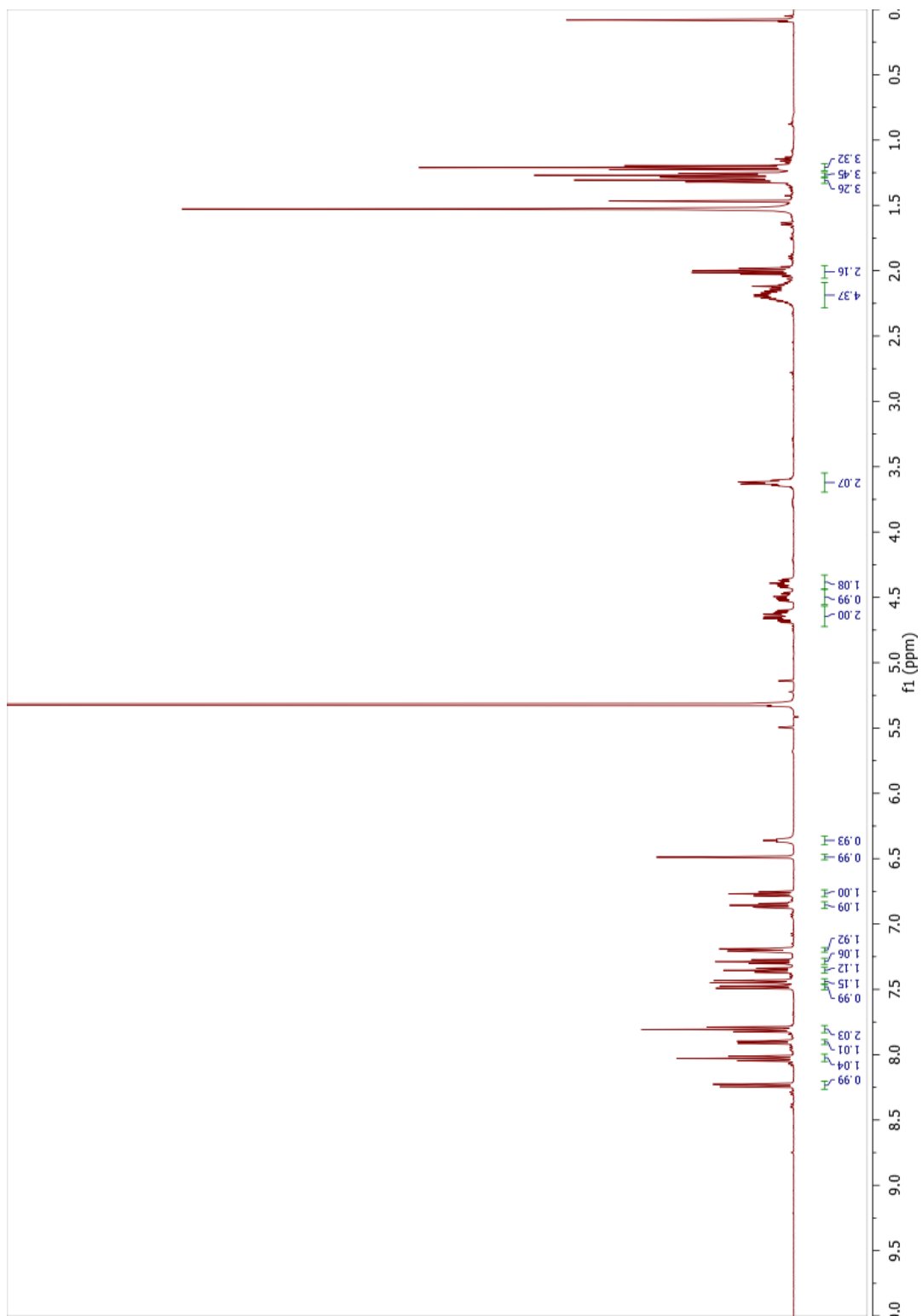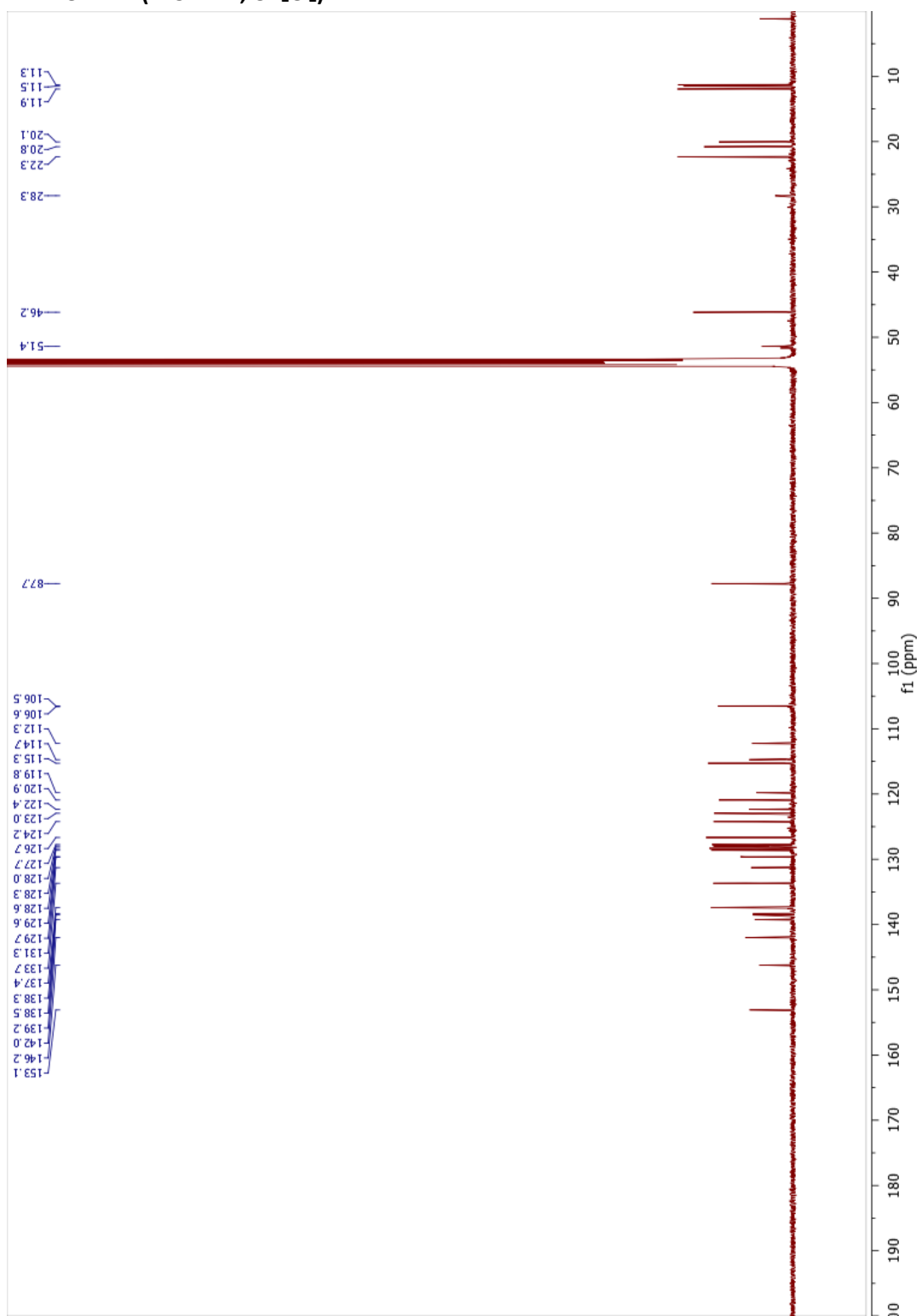
### 3.4.3.3    $^{19}$F NMR (282 MHz, CD$_2$Cl$_2$)

-152.22
-152.17

f1 (ppm)
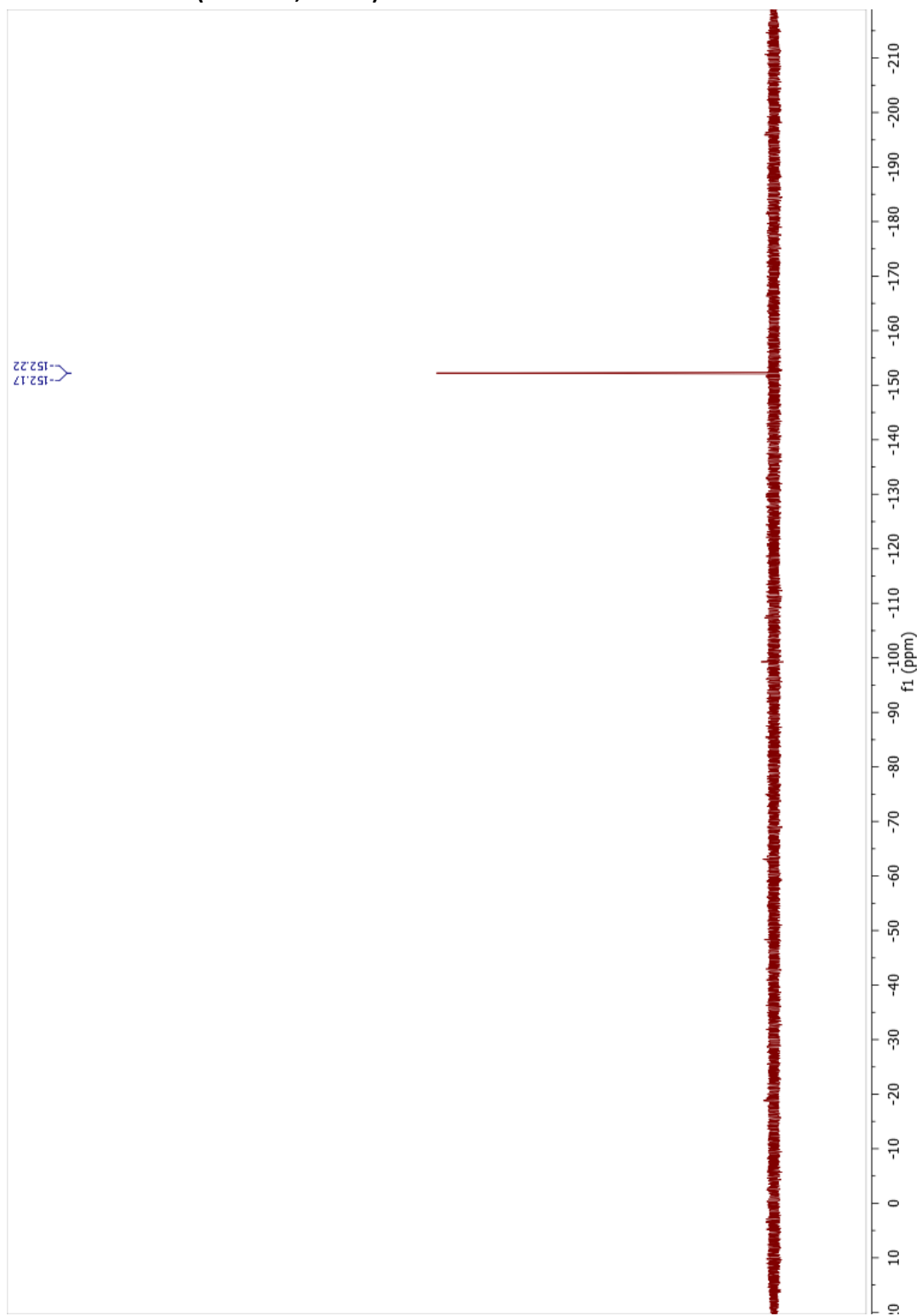
### 3.4.3.4 IR (neat, cm-1)
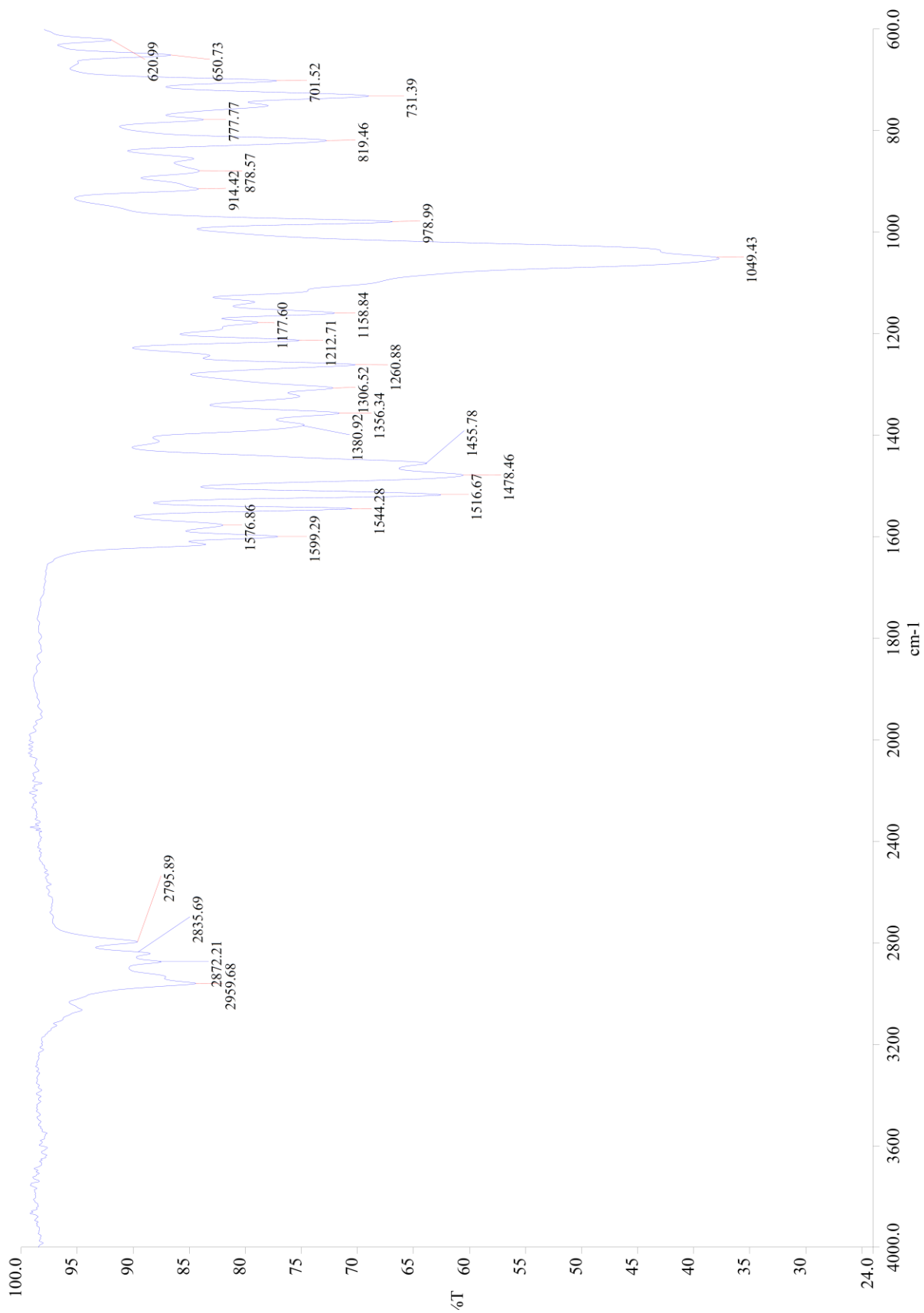
### 3.4.3.5 HRMS (ESI)

**UNIVERSITY OF GENEVA**

Faculty of Sciences

Sciences Mass Spectrometry

| | | | |
|---|---|---|---|
| Submitter: | BOSSON | Date of reception: | 21/07/14 |
| Sample name: | JB326 | Date of certificate: | 22/07/14 |
| Sample number: | 7357 | Data filename: | SMS10GE-140721-ES-A002 |
| Operator: | Eliane Sandmeier | Instrument: | QSTAR Pulsar (AB/MDS Sciex) |
| Principal investigator: | Dr. Sophie Michalet | Ionisation mode: | ESI (positive mode) |

| Expected Formula | Observed $m/z$ [M]$^+$ | Expected $m/z$ (amu) | Accuracy (ppm) |
|---|---|---|---|
| $C_{36}H_{36}N_3$ | 510.2899 | 510.2904 | -0.9 |

JB326





Spectrum from SMS10GE-140721-ES-A002.wiff (sample 13) - 7357, +TOF MS (100 - 2500) from 1.050 min, Recalibrated
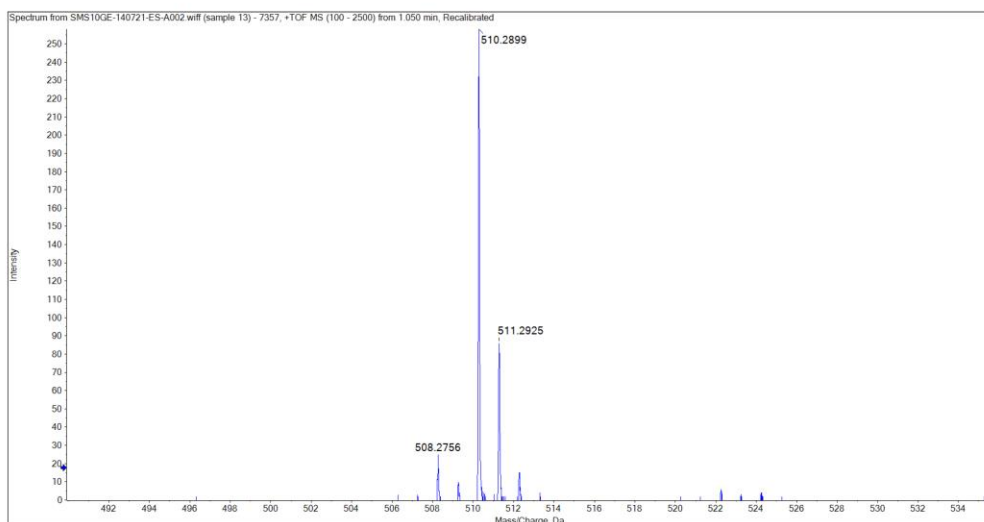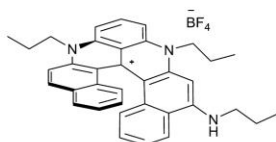
# 4  Calculations

## 4.1  Calculation methods

DFT and TD-DFT calculations on molecules were carried out with the latest version of the Gaussian 09.D01 program,[14] applying both a tightened self-consistent field convergence criterion ($10^{-9}$-$10^{-10}$ au) and an improved optimization threshold ($10^{-5}$ au on average forces). For each molecule, we have first optimized the geometry of the ground electronic state and computed its vibrational spectra to ascertain the nature of the optimized structure. Next, the geometry and vibrational frequencies of the lowest singlet excited-state were determined with TD-DFT using analytical gradients and numerical Hessian methods, respectively. The same DFT integration grid, namely the so-called *ultrafine* pruned (99,590) grid, was used for all calculations. All DFT and TD-DFT structural calculations were performed with the M06-2X hybrid exchange–correlation functional[15] that is suited for calculations of dyes with a cyanine character.[16,17] The CT parameters (see below) and MOs have been determined with the same functional. While structural parameters were determined with the 6-31G(d) atomic basis set, transition energies have been obtained with the more extended 6-311+G(2d,p) atomic basis set. Bulk solvation effects (here acetonitrile) have been systematically taken into account using the Polarizable Continuum Model (PCM).[18] The structural and vibrational parameters of the excited-state were obtained in the linear-response (LR) PCM model,[19] considering the so-called *equilibrium* limit. To determine the absorption and emission energies, we have applied the corrected LR (cLR) PCM approach[20] in its *non-equilibrium* limit as this protocol is suited to investigate electronic transitions. We have determined $\Delta\rho$ plots and associated charge-transfer (CT) parameters following the procedure defined by Le Bahers and coworkers.[21]

CC2 transition energies have been determined using the Turbomole package[22] applying the so-called resolution-of-identity (RI) approximation and correlating all electrons (no frozen-core). These calculations use the *aug*-cc-pVDZ atomic basis set and default convergence thresholds.

The 0-0 energies reported in the main text have been obtained by a composite protocol in which the structures and vibrational contributions are determined with (TD-)DFT using the above-described protocols, whereas the total transition energies are obtained at the CC2 level. The solvent effects are added by determining the differences between cLR-PCM and gas-phase TD-DFT energies. This protocol has been detailed in a recent work to which we refer the interested readers.[23] Vibronic calculations have been performed using the FCclasses code,[24] applying the Franck-Condon approximation.[25] The reported spectra have been simulated by using convoluting Gaussian functions that represent a half-width at half-maximum (HWHM) of 0.06 eV that allows accurate comparisons with experimental results (values specified in captions). A maximum number of 25 overtones for each mode and 20 combination bands on each pair of modes were included in the calculation. We note that, to consistently compare experimental and calculated spectra, the experimental spectra measured in the wavelength scale have been transformed in line shapes following published procedures to allow comparisons in this ESI (Figure S28).[26]

## 4.2    Extra vibronic data



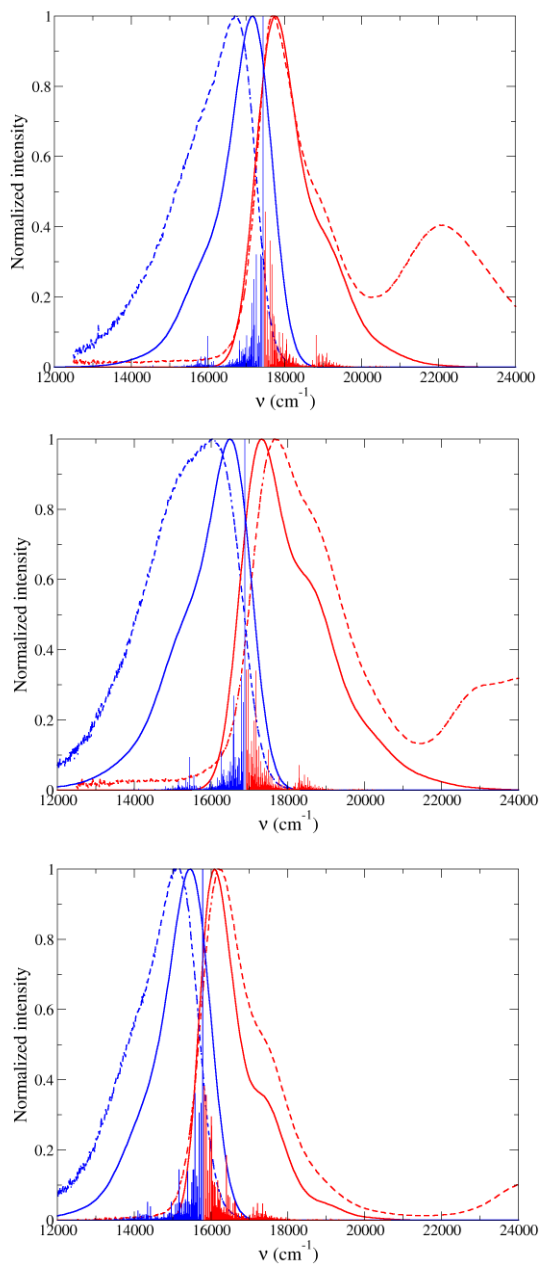Figure S25. Comparison between experimental (dotted curves) and theoretical (straight curves) fluorescence (blue) and absorption (red) lineshapes for **1** (top), **2** (center) and **3** (bottom). Note that the experimental spectra were transformed from nm to cm$^{-1}$, rescaled ($I_{abs}/\upsilon^3$ and $I_{em}/\upsilon^5$) and then normalized to obtain line shapes that can be meaningfully compared to theoretical calculations.

| | Absorption | | | |
|---|---|---|---|---|
| | Mode n° | Characteristics | Freq. (cm$^{-1}$) | Rel. Int. |
| **1** | 3 | Na rings *s/b* | 17499 | 0.44 |
| | 8 | Na C-C *t* | 17612 | 0.35 |
| | 11 | Na/Ph rings *t* and Na ring *r* | 17673 | 0.29 |
| | 91 | C-C rings *as* (breathing) | 18821 | 0.09 |
| **2** | 1 | Na(O) & N-ring *w* and Na(N) *r* | 16920 | 0.34 |
| | 5 | Na(O) & N-ring t and Na(N) *r* | 16966 | 0.34 |
| | 14 | Na(O), O, P *t* and Na(N) *r* | 17159 | 0.34 |
| | 37 | Na(O), O, P *t* and Na(N) *r* | 17491 | 0.11 |
| | 98 | C-C rings *as* (breathing) | 18287 | 0.07 |
| **3** | 1 | *Na(N) & N-ring w* and Na(N) *r* | 15821 | 0.38 |
| | 5 | *Na(N) & N-ring t* and Na(N) *r* | 15870 | 0.36 |
| | 12 | CH$_3$ *r* | 16000 | 0.29 |
| | 40 | Na, O, P *t* and Na *r* | 16392 | 0.18 |
| | 105 | C-C rings *as* (breathing) | 17206 | 0.05 |
| | 119 | N-P-N nodes *as* | 17335 | 0.05 |

Table S4. Vibronic analysis of the key vibrational modes explaining the vibronic couplings. Na(O or N), O, N, P stands for Naphtalene ring(besides O or N rings), O containing ring, N containing ring and Phenyl ring, respectively. *Ss*, *as*, *s/b*, *r,w* and *t* indicate for symmetric stretching, asymmetric stretching, scissoring/bending, rocking, wagging and twisting vibrational modes, respectively. See also Figure S29 for representation.
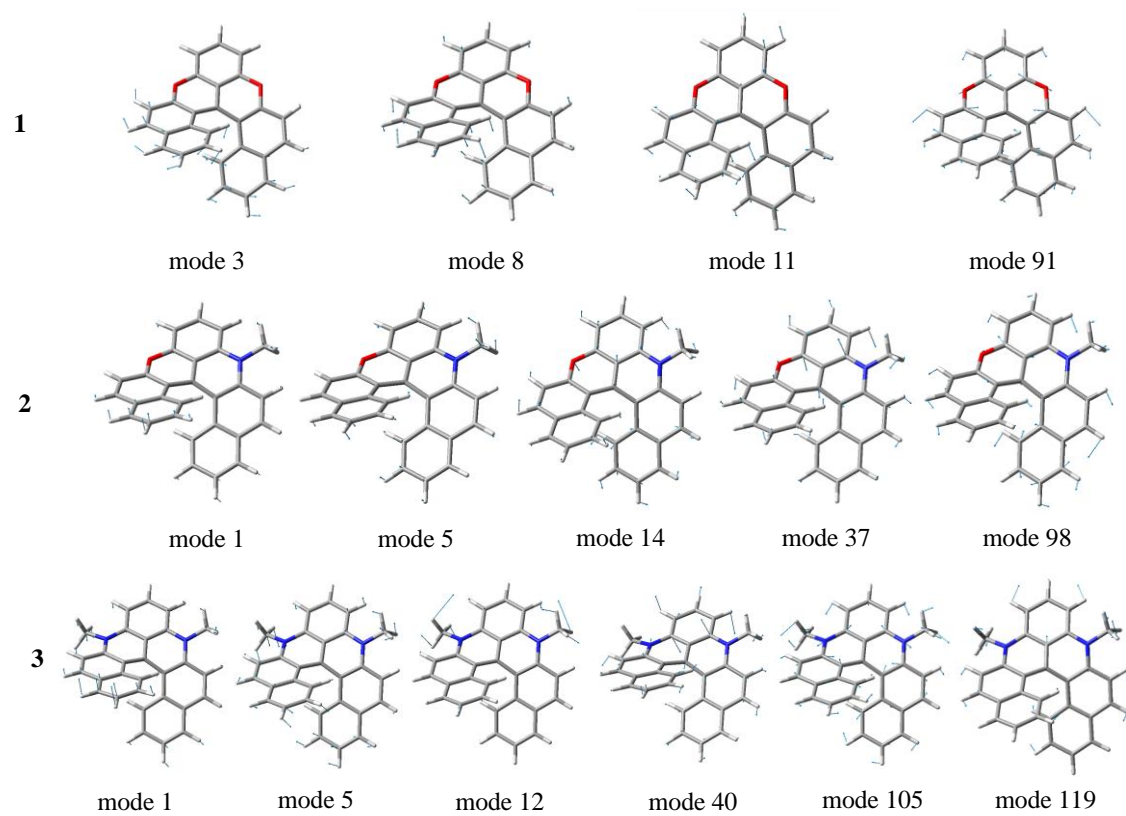
mode 3     mode 8     mode 11     mode 91

mode 1     mode 5     mode 14     mode 37     mode 98

mode 1     mode 5     mode 12     mode 40     mode 105     mode 119

Figure S26. Key vibrational modes listed in Table S4.

# 5   References

[1] B. W. Laursen, F. C. Krebs, *Chem. Eur. J.* **2001**, *7*, 1773-1783.

[2] B. W. Laursen, F. C. Krebs, *Angew. Chem. Int. Ed.* **2000**, *39*, 3432-3434.

[3] P. A. Muller, C. Högemann, X. Allonas, P. Jacques, E. Vauthey *Chem. Phys. Lett.* **2000**, *326*, 321-327.

[4] A. Fürstenberg, E. Vauthey *Photochem. Photobiol. Sci.* **2005**, *4*, 260-267.

[5] A. Morandeira, L. Engeli, E. Vauthey *J. Phys. Chem. A* **2002**, *106*, 4833-4837.

[6] G. Duvanel, J. Grilj, H. Chaumeil, P. Jacques, E. Vauthey *Photochem. Photobiol. Sci.* **2010**, *9*, 908-915.

[7] G. Duvanel, N. Banerji, E. Vauthey *J. Phys. Chem. A* **2007**, *111*, 5361-5369.

[8] N. Banerji, G. Duvanel, A. Perez-Velasco, S. Maity, N. Sakai, S. Matile, E. Vauthey *J. Phys. Chem. A* **2009**, *113*, 8202-8212.

[9] B. Lang, S. Mosquera-Vazquez, D. Lovy, P. Sherin, V. Markovic, E. Vauthey *Rev. Sci. Instrum.* **2013**, *84*, 073107-073108.

[10] O. Yushchenko, R. V. Hangarge, S. Mosquera-Vazquez, S. V. Bhosale, E. Vauthey *J. Phys. Chem. B* **2015**, *119*, 7308-7320.

[11] E. Brunet, L. Jiménez, M. de Victoria-Rodriguez, V. Luu, G. Muller, O. Juanes, J. C. Rodríguez-Ubis, *Microporous Mesoporous Mater.* **2013**, *169*, 222, and references therein.

[12] H. P. J. M. Dekkers, P. F. Moraal, J. M. Timper, J. P. Riehl, *Appl. Spectrosc.* **1985**, *39*, 818-821.

[13] F. Torricelli, J. Bosson, C. Besnard, M. Chekini, T. Bürgi and J. Lacour, *Angew. Chem. Int. Ed.* **2013**, *52*, 1796-1800.

[14] Frisch, M. J.; Trucks, G. W.; Schlegel, H. B.; Scuseria, G. E.; Robb, M. A.; Cheeseman, J. R.; Scalmani, G.; Barone, V.; Mennucci, B.; Petersson, G. A.; Nakatsuji, H.; Caricato, M.; Li, X.; Hratchian, H. P.; Izmaylov, A. F.; Bloino, J.; Zheng, G.; Sonnenberg, J. L.; Hada, M.; Ehara, M.; Toyota, K.; Fukuda, R.; Hasegawa, J.; Ishida, M.; Nakajima, T.; Honda, Y.; Kitao, O.; Nakai, H.; Vreven, T.; Montgomery, J. A., Jr.; Peralta, J. E.; Ogliaro, F.; Bearpark, M.; Heyd, J. J.; Brothers, E.; Kudin, K. N.; Staroverov, V. N.; Kobayashi, R.; Normand, J.; Raghavachari, K.; Rendell, A.; Burant, J. C.; Iyengar, S. S.; Tomasi, J.; Cossi, M.; Rega, N.; Millam, J. M.; Klene, M.; Knox, J. E.; Cross, J. B.; Bakken, V.; Adamo, C.; Jaramillo, J.; Gomperts, R.; Stratmann, R. E.; Yazyev, O.; Austin, A. J.; Cammi, R.; Pomelli, C.; Ochterski, J. W.; Martin, R. L.; Morokuma, K.; Zakrzewski, V. G.; Voth, G. A.; Salvador, P.; Dannenberg, J. J.; Dapprich, S.; Daniels, A. D.; Farkas, Ö.; Foresman, J. B.; Ortiz, J. V.; Cioslowski, J.; Fox, D. J. Gaussian 09, revision D.01; Gaussian, Inc.: Wallingford, CT, 2009.

[15] Y. Zhao and D. G. Truhlar, *Theor. Chem. Acc.*, **2008**, *120*, 215-241.

[16] D. Jacquemin, Y. Zhao, R. Valero, C. Adamo, I Ciofini, D. G. Truhlar, *J. Chem. Theory Comput.*, **2012**, *8*, 1255-1259.

[17] B. Le Guennic and D. Jacquemin, *Acc. Chem. Res.*, **2015**, *48*, 530-537.

[18] J. Tomasi, B. Mennucci and R. Cammi, *Chem. Rev.*, **2005**, *105*, 2999-3094.

[19] (a) R. Cammi and B. Mennucci, *J. Chem. Phys.*, **1999**, *110*, 9877-9886; (b) M. Cossi and V. Barone, *J. Chem. Phys.*, **2001**, *115*, 4708-4717.

[20] M. Caricato, B. Mennucci, J. Tomasi, F. Ingrosso, R. Cammi, S. Corni and G. Scalmani, *J. Chem. Phys.*, **2006**, *124*, 124520.

[21] (a) D. Jacquemin, T. L. Bahers, C. Adamo and I. Ciofini, *Phys. Chem. Chem. Phys.*, **2012**, *14*, 5383-5388; (b) T. Le Bahers, C. Adamo and I. Ciofini, *J. Chem. Theory Comput.*, **2011**, *7*, 2498-2506.

[22] Turbomole V6.6 2014, a Development of University of  Karlsruhe and Forschungszentrum Karlsruhe GmbH, 1989–2007, Turbomole GmbH. http://www.turbomole.com [last accessed 19.06.16]

[23] D. Jacquemin, I. Duchemin, X. Blase, *J. Chem. Theory Comput.*, **2015**, *11*, 5340-5359.

[24] F. Santoro, FCclasses, A Fortran 77 Code, 2011. See: http://village.pi.iccom.cnr.it [last accessed 10.07.13].

[25] (a) F. Santoro, R. Importa, A. Lami, J. Bloino, V. Barone, *J. Chem. Phys.*, **2007**, *126*, 084509; (b) F. Santoro, A. Lami, R. Importa, V. Barone, *J. Chem. Phys.*, **2007**, *126*, 184102.

[26] F. J. Avilla Ferrer, J. Cerezo, E. Stendardo, R. Improta, F. Santoro, *J. Chem. Theory Comput.*, **2013**, *9*, 2072-2082.